(343)

FINAL TECHNICAL REPORT
PAKISTAN SCIENCE FOUNDATION

Project Title:	Wave Propagation and Transport Phenomenon in Controlled Fusion
Name of Principal Investigator:	Professor Dr. G. Murtaza
Name and Address of Reporting Institution:	Department of Physics Quaid-i-Azam University Islamabad.
Project Number:	PSF/Res/C-QU/Phys(69)

Signature of Principal Investigator: G Murtaza

Principal Investigator
Project C-QU/Phys (69)
Quaid-i-Azam University
ISLAMABAD

Signature of the Institutional Head:

Vice-Chancellor
Quaid-i-Azam University
Islamabad

SUMMARY OF THE PROJECT

Title: Wave Propagation and Transport Phenomenon in Controlled Fusion

In the project under consideration, which was for a period of three years, we have dealt with the following problems.

i) The dynamics of a finite-thickness gas-puff $Z-\theta$ pinch producing a high density plasma was investigated and studied numerically. The results obtained by modifying the codes of earlier work have been published in an international journal (see copy attached). Considering the effect of Ohmic heating with adiabatic conditions and incorporating the radiation losses, fusion conditions were studied for a finite-thickness gas-puff staged Z-pinch. The results of this study have been accepted for publication (see copy attached). An important observation was made that a relatively thick puff layer will be useful to obtain parameters like density and temperature with enhanced stability in the acceleration phase of puff layer in contrast with the theoretical observations of the previous work advocating thin puff layer.

The numerical results we have obtained predict stability and will be very helpful in future experimental work on $Z-\theta$ pinch device in our plasma laboratory.

ii) Regarding work on laser-induced plasma, an analytical nonlocal heat transport formula based on the reduced Fokker-Planck equation was considered. The effects of inverse-bremsstrahlung absorption as well as the electrostatic po-

tential on heat flux for a strongly inhomogeneous plasma were investigated. It was found that while the former contributes an additive term to the heat flux enhancing its value for both steep and gentle gradient situations; the latter effect introduces an exponential term which significantly reduces the electron thermal transport. Our calculations also showed that for a moderately intense laser field, the maximum heat flux for steep gradient situations corresponds to flux inhibition factor of the order of 0.17. This work has also been published (see copy attached).

iii) Experimental work on sequential focusing in a Mather-type Plasma Focus has been carried out. The results indicate that such a device can possibly be used as a cascading focus device to produce bursts of neutrons and soft x-rays. This work has been published in a journal of international repute (see copy attached).

INTRODUCTION

Research on production and containment of high density, high temperature plasma has been going on for some years in order to achieve controlled thermonuclear fusion. The controlled thermonuclear fusion has been acknowledged to be the long term pollution-free source of energy. It is also recognized to be less hazardous as compared to fission.

a) Dynamics of $Z - \theta$ pinch.

Since the beginning of controlled thermonuclear fusion, research on fast pinches has been the focus of attention. The two simplest types of plasma pinches that have been studied over the years are Z-pinches and θ- pinches. In these pinches, a pulse current flows through a cylindrical column of the neutral gas that ionizes and heats the gas by ohmic dissipation. This plasma column then collapses on the axis due to the pressure of self-generated magnetic field. It has been realized quite early that the pinches are plagued with instabilities that appear both during the run in phase, Rayleigh-Taylor type instabilities, and in the collapse phase, Sausage and Kink instabilities. Because of these instabilities, the collapse is non-uniform and the plasma column breaks up prematurely. Formation of hot spots and the generation of neutrons are normally attributed to these instabilities. A novel method of suppressing some of the instabilities particularly the running phase instabilities and the formation of the dense Z-pinches was proposed [1, 2] and investigated experimentally [3, 4]. In this method dense Z-pinches are formed from frozen deuterium fibers, through which rapidly rising currents are driven by means of modern low impedance pulse generators. In all these experiments, it is seen that the fiber plasma column expands during the

rise time of the pulse that may be due to its slow rise time. It is also found [4] that the pinch is stable as long as $\frac{dI}{dt} > 0$ and becomes unstable at the peak of the current profile i.e. at $\frac{dI}{dt} = 0$. It was also realized and confirmed by experiments that much higher value of $\frac{dI}{dt}$ is required, to avoid expansion of the plasma column, than can be delivered by even the most modern pulse generators. On the other hand it seems that even this scheme can not avoid the growth of MHD instabilities particularly the Sausage instability. However, efforts are underway to build a generator that will produce much larger values of the peak currents with significantly higher values of $\frac{dI}{dt}$. To overcome the two problems mentioned above, namely the requirement for large $\frac{dI}{dt}$ and instabilities, a completely different method of forming a dense plasma column was proposed that also initiates from solid fiber [5, 6].

This method is based upon the hybrid concept of Z and θ-pinch and is called $Z - \theta$ pinch or staged Z-pinch. The $Z - \theta$ pinch consists of a simple gas-puff Z-pinch with an additional axial magnetic field B_z due to the azimuthal current J_θ produced by the Helmholtz coils. The schematic diagram of the device is given in Fig.(1) and the principle is as follows: according to this scheme a hollow annular gas column is puffed between two electrodes of the Z-pinch. A small, solid quartz fiber or hollow parylene straw is placed co-axial with the gas-puff as shown in Fig.(1). Before the electrodes are energized by a capacitor bank C_0, Helmholtz coils generate an axial magnetic field $\vec{B}_z$. When C_0 is discharged, the $\vec{J}_z$ current between the electrodes increases and the annular plasma implodes to a small radius by the action of the $\vec{J}_z \times \vec{B}_\theta$ self magnetic force. Due to the high conductivity of the annular Z-pinch plasma, the $\vec{B}_z$ gets trapped and compressed

to extremely high levels on a time scale much faster than the driving current of the Z-pinch. This rapidly rising magnetic field $\vec{B}_z$ induces the azimuthal current $\vec{J}_\theta$ on the surface of the fiber or the straw. Due to the Ohmic dissipation, this current may heat the material to very high temperature turning it to a very high density plasma. Depending on the magnitude of the induced current the plasma can also implode by the $\vec{J}_\theta \times \vec{B}_z$ force. The formation and heating of this high energy density plasma happens so fast that the losses due to radiation can be ignored on the time scale of the implosion, leading it to an extremely high energy density plasma. This configuration also provides more stability to the plasma as compared to Z-pinch and θ-pinch alone.

In earlier experiments on the same facility at the University of California, Irvine (UCI) [7], the compressed magnetic field was measured to be 1.6MG for r_0 = 2cm, B_0 = 9KG. Subsequent experiments have reported 2.5MG in the USSR [8, 9] and 40MG at Sandia National Laboratories [10]. In these experiments high compression was achieved by using the high Z gases such as Kr and Xe.

The $Z-\theta$ pinch is a novel method of producing the ultrahigh magnetic fields in a controlled manner with high repetition rate. Since this method is free from explosion or material deformation, it can produce many successive plasma pinches without breaking the vacuum. The $Z-\theta$ pinch has potential applications in X-ray lasers, thermonuclear fusion, gamma-ray generators and atomic physics studies [11].

The $Z-\theta$ pinch plasma dynamics problem can be divided into two parts namely the outer gas shell dynamics and the DT-fiber or straw dynamics.

Plasma pushing by magnetic pressure is an important process in many laboratory plasmas. The simplest model which describes this pushing is the Snow-plow model. If a fully ionized plasma is considered as a perfect conductor, the initial discharge current would flow on the outer surface of the plasma, parallel to the axis of the cylinder in the form of a current sheath which sets up an azimuthal magnetic field $\vec{B}_\theta$ just outside the current layer. Since there is no field inside the gas-puff plasma, the sheath experiences an inward pressure $\frac{B_\theta^2}{8\pi}$ and so begins to contract. As it moves inward, the current sheath behaves like a magnetic piston and sweeps up all the plasma particles it encounters. This is the so called the Snow-plow model.

Rahman et al., [6] modified the usual Snow-plow model to describe the dynamics of outer Z-pinch which involves the implosion of the annular plasma shell that pinches the entrained axial magnetic field. Rahman et al., neglected the thickness of the annular plasma shell in their model. Since in most of the experiments gas-puff has finite thickness, theoretical modeling for such a $Z-\theta$ pinch is in order. For finite thickness gas-puff, the Snow-plow effect would occur in the puffed region, it would move then like a thin constant mass layer, as described by Rahman et al.

The effect of finite-thickness gas-puff on the dynamics of outer Z-pinch has been investigated by using Snow-plow model [12]. Our results indicate that for thick gas-puff layer fast compression occurs whereas, for a very thin puff layer earlier results of Rahman et al. hold. Fast compression has the additional advantage of pinch stability and ultrahigh axial magnetic field on a time scale of the order of current rise time.

The same problem has been extended [13] to study the dynamics of inner θ-pinch by assuming a uniform column of high density plasma. The Ohmic and adiabatic heating and cyclotron and bremsstrahlung radiation losses are also taken into account. The numerical results obtained are shown in Figs. (4,5).

b) Laser induced plasma.

The success of laser-induced fusion through compression of a spherical tiny target to super-high density depends upon laser energy absorption in the underdense region and then its efficient transfer from the lower density corona to a higher density ablation surface. It is important to directly heat as many electron as possible, but at the same time avoid generation of suprathermal electrons which can penetrate the core of the target before the final compression occurs. Since in laser fusion, the laser energy is continuously being deposited at the top of the heat front and absorbed by the thermal electrons, a self-consistent treatment of the absorption process and the heat transport is in order. The most effective absorption mechanism for high Z-plasmas is the collisional inverse-bremsstrahlung process. This process leads to a slight overestimation of the absorption and of the transport itself. Albritton [14], used a simplified high-Z diffusion approximation of the Fokker-Planck equation to study the heat transport in laser produced plasmas and the Langdon [15] effect was taken into account to simulate the inverse-bremsstrahlung absorption process.

There is a general consensus that the problem of heat transport under steep gradients produced by intense laser beam becomes nonlocal [16, 17], and that the isotropic part of the distribution function, f_0, cannot be taken to be a local Maxwellian. Attempts have been made to study the steep temperature gradi-

ent situations by numerically solving the kinetic Fokker-Planck equation including electron-electron, electron-ion, and inverse-bremsstrahlung absorption terms. But this approach seems to be very time-consuming and therefore, in most of the hydrodynamics codes, one generally uses simplified numerically efficient nonlocal models. In addition a number of analytical models based on the solution of kinetic Fokker-Planck equation have been proposed. Later the effect of electrostatic potential on nonlocal heat transport was studied by Mirza et al. [18] by solving the reduced Fokker-Planck equation but ignoring the inverse-bremsstrahlung term. On the other hand, Luciani and Mora [19] have proposed a nonlocal heat transport model which incorporated the inverse-bremsstrahlung absorption effect but did not include self-consistently the electrostatic potential effect.

The previous nonlocal model [18] has been extended by solving the reduced Fokker-Planck equation with the local inverse-bremsstrahlung absorption term [20]. Its effect on nonlocal heat transport is investigated schematically. The limiting cases for steep and gentle gradients are found to be modified and the ensuing results show good agreement with simulations of the kinetic Fokker-Planck equation possessing the inverse-bremsstrahlung absorption term.

c) Experimental work on plasma Focus.

On experimental side, work is done on the low energy Mather-type plasma focus system, which is energized by a single $32\mu F$, $15KV$ $(3.6KJ)$ capacitor. The electrodes of the device consist of a $152mm$ long Cu rod of $18mm$ diameter as anode, surrounded by six cathode rods of thickness $10mm$ forming a co-axial system. The cathode rods are screwed to a Cu plate with a knife edge near the anode. An insulator sleeve of Pyrex glass, $25mm$ in length from the cathode base

plate, is placed between the anode and cathode. A $13mm$ thick rubber disc with a hole at its centre is used to support the cylindrical glass sleeve, so that it can be positioned without touching the anode or the cathode. The electrode system is enclosed in a vacuum chamber which may be evacuated up to $5 \times 10^{25} mb$. A swinging cascade type open air spark gap made of 1/2 inch thick Cu plate was employed to transfer energy from the capacitor to the electrodes of the device.

When high voltage is applied, dielectric breakdown of the filling gas occurs between the electrodes via insulator sleeve surface. As a result of this process, current sheath formation is initiated which expands radially and starts moving towards open end of the accelerator due to the magnetic pressure behind the current sheath. The lengths of the electrodes and the filling pressure are adjusted in such a manner that the current through the device is maximum when current sheath reaches at the open end of the accelerator. At this instant radial collapse of the current sheath occurs resulting in the formation of high density and high temperature focus plasma just beyond the face of central electrode. When the device is operated with D_2 or deuterium and tritium mixture as the filling gas, intense bursts of neutrons and X-rays are emitted from the focus region. The effects of the target placed downstream anode have been studied [22].

RESULTS

The $Z-\theta$ pinch dynamics based on the Rahman et al., model [6] has been studied in which the implosion of an annular gas-puff of negligible thickness was considered. However, in experimental point of view, the gas-puff has always some finite thickness. The Snow-plow effect can be incorporated to describe the dynamics of an imploding annular plasma shell of finite-thickness. A dynamic model [12] for a finite thickness gas-puff $Z-\theta$ pinch has been proposed. The numerical simulation of this problem has been performed for different values of the puff-thickness L_p. Fig.(2) shows the variation of imploding plasma radius with time for various gas-puff thicknesses. The numerical results showed that for a thin gas-puff layer ($L_p \sim 0.01r$) the Rahman et al., model works very well and the current sheath moves like a constant mass layer. For $L_p \sim 0.01r$, maximum compression has been obtained (corresponding to minimum radius $R \sim 0.1$) after a time of the order of 1.1 times the current rise time. On the other hand, for puff thickness ($0.01 < L_p/r < 0.99$) the compression occurs at an earlier time. For $L_p \sim r$, the plasma radius reaches its maximum compression in time $\sim 0.94t$. It has been found that for puff thicknesses $L_p > 0.1r$, all the R vs τ curves converge to the curve corresponding to time $0.94t$. For all values of puff thicknesses, the compression time of the imploding plasma radius is an order of magnitude less than the current rise time. As the plasma column implodes, it compresses the magnetic field to high strengths. Fig.(3) exhibits how the axial magnetic field varies in time for different values of the puff thickness. Maximum magnetic field of about $100MG$ is obtained for a very thin puff layer i.e., $L_p \sim 0.01r$. As the puff thickness increases, the value of the magnetic field decreases. For $L_p \sim r$,

the magnetic field is of the order of $70MG$. For thick gas-puff, the axial magnetic field peaks up in small time scale.

The effect of finite-thickness gas-puff on the dynamics of inner θ-pinch has been investigated by incorporating the Ohmic and adiabatic heating and cyclotron and bremsstrahlung radiation losses [13]. For very thin-puff layers, the earlier results of Rahman et al. are completely recovered i.e., maximum compression takes place at 53.6 nsec. with $n \sim 5 \times 10^{25} cm^{-3}$ and $T \sim 70keV$. Note that the current rise time t_0 is 50 nsec. and thus the maximum compression for a very thin puff layer occurs after the current peaks. On the other hand, for a relatively thick puff layer, the maximum compression values of $n \sim 1.5 \times 10^{25} cm^{-3}$ and $T \sim 30keV$ are achieved earlier than the current rise time. Fig.(4) displays the results for the inner θ-pinch D-T plasma i.e., the temporal variation of the plasma radius a, the density n and the temperature T for various puff thicknesses. The curves for a, n and T converge to the same curve corresponding to the time around 44.2 nsec thus obviating the necessity of increasing puff-thickness.

In laser produced plasma, an analytical nonlocal heat transport formula has been derived from the reduced Fokker-Planck equation including inverse-bremsstrahlung absorption as well as the electrostatic potential. It is found that the inverse-bremsstrahlung contributes an additional term to the heat flux and enhances its value for both steep- and gentle- gradient situations. The electrostatic potential introduces an exponential term which significantly reduces the electron thermal transport. It is also found that for a moderately intense laser field, the maximum heat flux for steep gradient situations corresponds to flux inhibition factor $f \sim 0.15 - 0.17$.

The experiments were carried out in a low energy plasma focus device energized by a single capacitor. The effects of the target placed down stream the anode on the neutron yield and the focusing action have been studied [22]. The target was a Cu disc having thickness of 5 mm and a diameter of 35 mm. It has been observed that thickness of the target has a crucial role since the current sheath, after climbing the target, must have sufficient time to become uniform before reaching the subsequent focusing event. The target is hanged from the top flange of the chamber with the help of two supporting rods. These supporting rods are 3 mm thick brass rods encapsulated in glass tubes. The target can be moved up and down without interrupting the vacuum in the chamber. The target insertion mechanism allows enough room to the current sheath to focus beyond the target.

A simple resistor divider has been employed to measure the transient voltage across the anode and cathode header. The average neutron yield is measured by indium foil activation detector. The neutron pulse was recorded by using the Integral Detector Assembly of NE Technology Limited whose signal was recorded on the dual channel digital oscilloscope.

In Fig.(6) average neutron yield as a function of the target distance from the anode tip is shown. It is clear that the neutron yield is independent of target position beyond 50 mm. However, placing the target closer to the anode surface decreases the average number of neutron counts and a minimum is obtained at a distance of about 2 cm. The reduction of neutron yield may be due to the interference of the target with the deuteron beam. This is confirmed by replacing the target with a copper disc of the same size having a 2 mm hole at its center

and this is shown in Fig.(6).

Interestingly, it is observed that by bringing the target even closer to the anode, the average neutron yield increases abruptly. Moreover a second spike is also observed in the high voltage probe signal and in the neutron pulse profile. This second spike is a clear indication of a second focus after the target. The second spike is relatively low in amplitude, indicating a weak focusing action. However, it proves that such a device can possibly be used as a cascading focus device to produce bursts of neutrons and soft X-rays.

DISCUSSION

In $Z-\theta$ pinch the compression at an earlier time would be very useful for stabilization. It may stabilize the Rayleigh-Taylor instability and the axial magnetic field generation on a time scale earlier than the current rise time [12]. The rapidly rising axial magnetic field would induce the azimuthal current J_θ on the surface of the fiber, then by Ohmic dissipation, this current would heat the material to very high temperature and density. This $Z-\theta$ pinch device can be used as a fusion reactor. The fast compression achieved by thick gas-puffs plays an important role in stabilization and this is consistent with the experimental observations of Hussey et al., in which they found that the evolution of the nonlinear Rayleigh-Taylor instabilities is qualitatively reduced for thick gas-puff layers. It is known that the Z-pinch plasma transfers its energy to the fiber at the time when the compression peaks. However, earlier model of thin shell gas-puff has shown that the imploding Z-pinch plasma approaches the minimum radius after the current peaks (i.e., when $dI/dt = 0$) and is believed to become highly unstable due to sausage instability, destroying the uniformity of the plasma column before the transfer of energy completes. In our model, on the other hand, the compression occurs before the current peaks and that might explain the stable formation in our case.

The Snow-plow effect incorporated in the Z-pinch dynamics also provides an additional stabilizing factor. In the acceleration phase of the outer Z-pinch plasma, the Rayleigh-Taylor instability is expected to occur which grows like $\xi = \xi_0 \exp(\gamma t)$ where $\gamma = (Kg)^{1/2}$ is the growth rate of instability. K is the wave number of the perturbation and $g = B_z^2/8\pi m$, m being the mass per unit area of

the Z-pinch. Since $S = gt^2/2$, one may obtain $\xi = \xi_0 \exp(2SK^{1/2})$, where S is the distance to which the Z-pinch is accelerated. The instability can be controlled by minimizing the values of the initial perturbation ξ_0, the distance S to which the Z-pinch is accelerated and the wave number $K = 2\pi/l$, where l is the shell thickness which increases due to the Snowplow effect. Thus a thick shell Z-pinch plasma is expected to be more stable than a thinner one.

In the laser produced plasma, the effect of inverse bremsstrahlung absorption on nonlocal heat transport has been investigated [18]. This effect is of fundamental importance in the laser plasma interaction experiments near the critical density surface since it determines the structure of the density and temperature profiles. It has been found that the inverse bremsstrahlung absorption effect enhances the heat flux (see Table 1). The same has also been observed in the Fokker-Planck numerical simulations of Matte et al. [21]. In the absence of local inverse bremsstrahlung absorption, the earlier results [18] are completely recovered. The comparison of our result with other nonlocal models is shown in Table 2.

CONCLUSIONS

The implosion of a dense θ-pinch plasma driven by an annular finite-thickness gas-puff Z-pinch is investigated numerically. The numerical results demonstrate that for a thick gas-puff layer, maximum compression occurs before the current peaks. It is also found that at peak compression, fuel density of the order of $10^{25} cm^{-3}$ and temperature greater than $10 keV$ can be achieved on a time scale of the order of $0.1 nsec$. Thus the Lawson parameter $n\tau \sim 10^{14} sec/cm^3$ for a D-T fiber becomes achievable. The Snow-plow effect in the Z-pinch exercises a stabilization effect on the growth of Sausage and Rayleigh-Taylor instability. In the limits of a very thin gas-puff layer, previous results are fully recovered.

In laser produced plasma, the effect of inverse-bremsstrahlung absorption on heat flux has been investigated. It is found that this absorption enhances the heat flux value which must be the case since the inverse-bremsstrahlung absorption mechanism provides thermal electron which mainly contributes the heat flux.

On the experimental side, the current sheath behavior in a small $3kJ$ plasma focus device, in the presence of a target placed downstream of the anode is investigated. The analysis of the voltage of the signal and the neutron pulse provides a clear indication of the sequential focusing. Such a device can be used as a cascading focusing device.

LIST OF PUBLICATIONS

Under this project, the following publications have been made.

1. **Theoretical Model for a Finite-Thickness Gas-puff $Z-\theta$ Pinch.**

   by

   Arshad M.Mirza, M.Iqbal, N.A.D.Khattak and G.Murtaza

   Modern Phys. Lett. B, **7**, 1655-1660, (1993).

2. **Fusion Conditions in a Finite-Thickness Gas-Puff Staged Z-Pinch**

   by

   Arshad M.Mirza, N.A.D.Khattak, M.Iqbal and G.Murtaza

   Journal of Plasma Phys., **(in press)**

3. **Role of Inverse Bremsstrahlung Absorption and Electrostatic Potential on Energy Transport Mechanism in Laser Produced Plasmas**

   by

   G.Murtaza, Arshad M.Mirza and M.S.Qaisar

   Physica Scripta **50**, 403-405, (1994).

4. **Sequential Focusing in a Mather-Type Plasma Focus**

   by

   M.Nisar, F.Y.Khattak, G.Murtaza, M.Zakaullah and N.Rashid

   Physica Scripta **47**, 814-816, (1993).

GRADUATE STUDENTS

The following two M.Phil. dissertations were based on the research work performed under the said project:

	Thesis Title	Author
1)	Effect of Parasitic Impurities on neutron Emission from a Low Energy Mather-type Plasma Focus.	Imtiaz Ahmad
2)	A Study Of $Z-\theta$ Pinch Dynamics.	M. Iqbal

LIST OF SCIENTISTS

1)	Prof.Dr.G.Murtaza	Principal Investigator
2)	Dr.M.Zakaullah	Assistant Professor
3)	Dr.Arshad M.Mirza	Assistant Professor
4)	Dr.F.Y.Khattak	PostDoc Fellow
5)	Dr.M.S.Qaisar	Senior Research Fellow
6)	Mr.M.Nisar	Ph.D. Scholar
7)	Mr.Imtiaz Ahmad	Research Officer/Ph.D. Scholar
8)	Mr.M.Iqbal	Research Officer/Ph.D. Scholar
9)	Mr.N.A.D.Khattak	Ph.D. Scholar
10)	Mr.N.Rashid	M.Phil. student

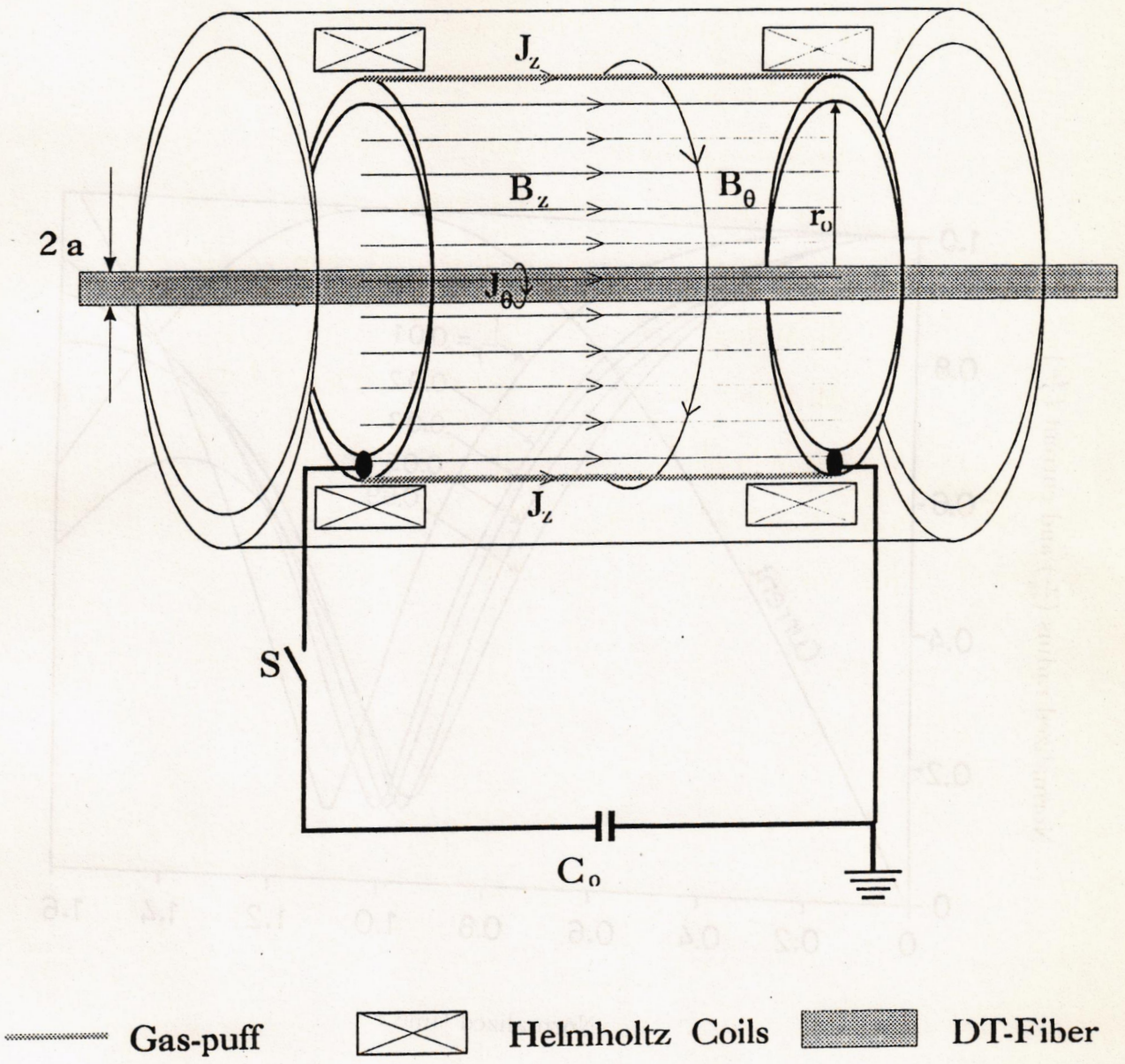

Figure 1: $Z - \theta$ pinch

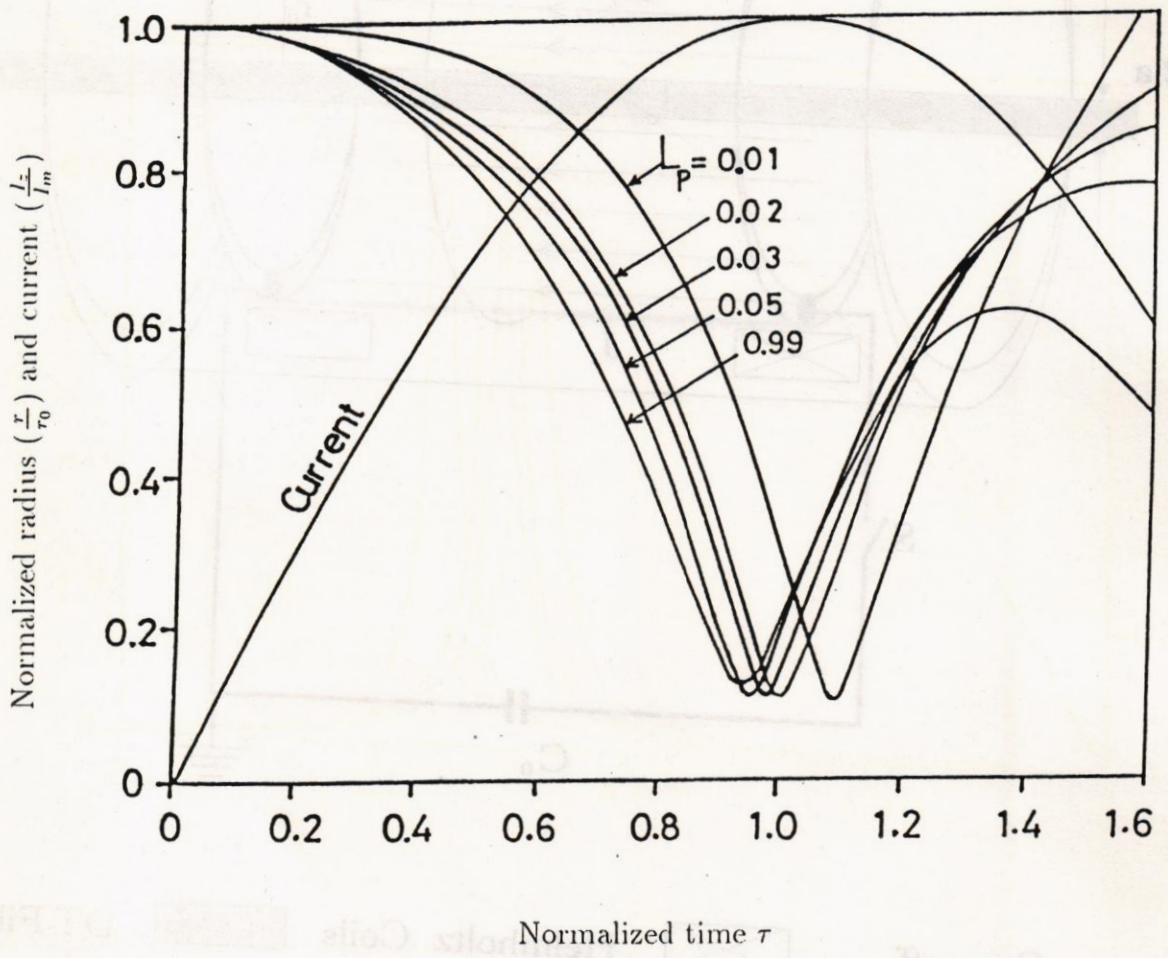

Figure 2: Normalized characteristics of $Z-\theta$ pinch with entrained axial magnetic field for various puff thicknesses with sinosoidal current profile

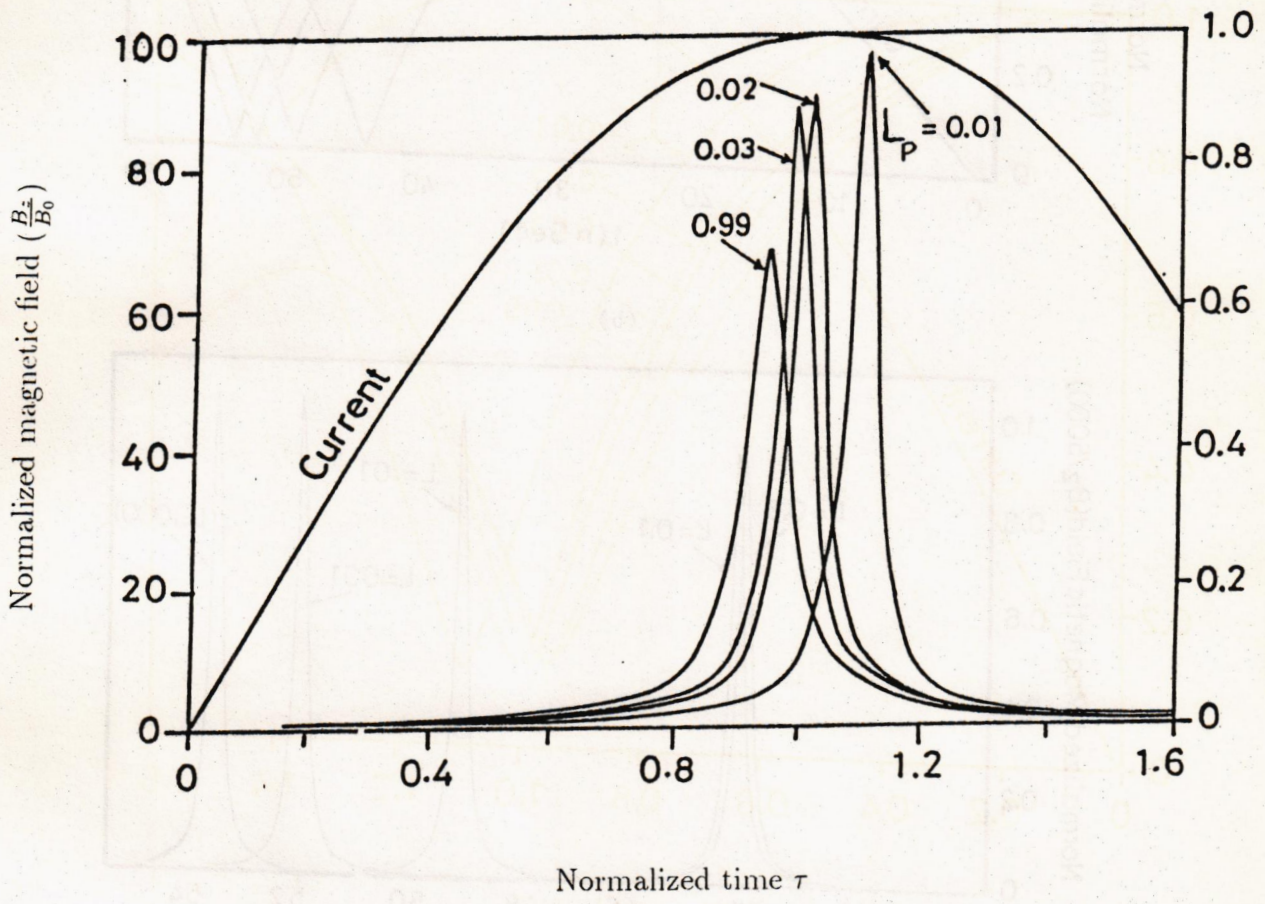

Figure 3: Normalized magnetic field viz normalized time for various gas-puff thicknesses with sinosoidal current profile

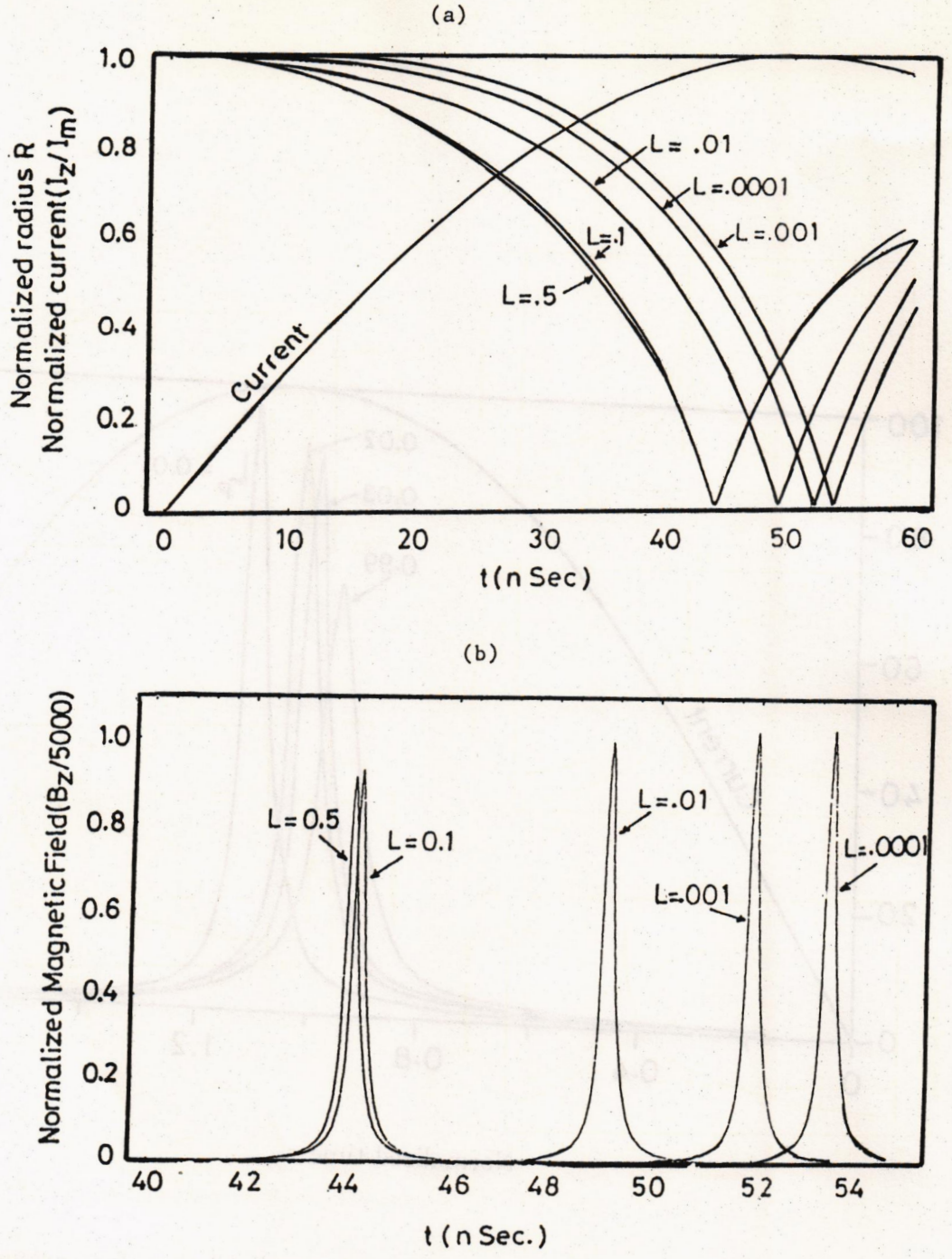

Figure 4: Radius and compressed magnetic field B_z (divided by 5000) for different puff thicknesses L

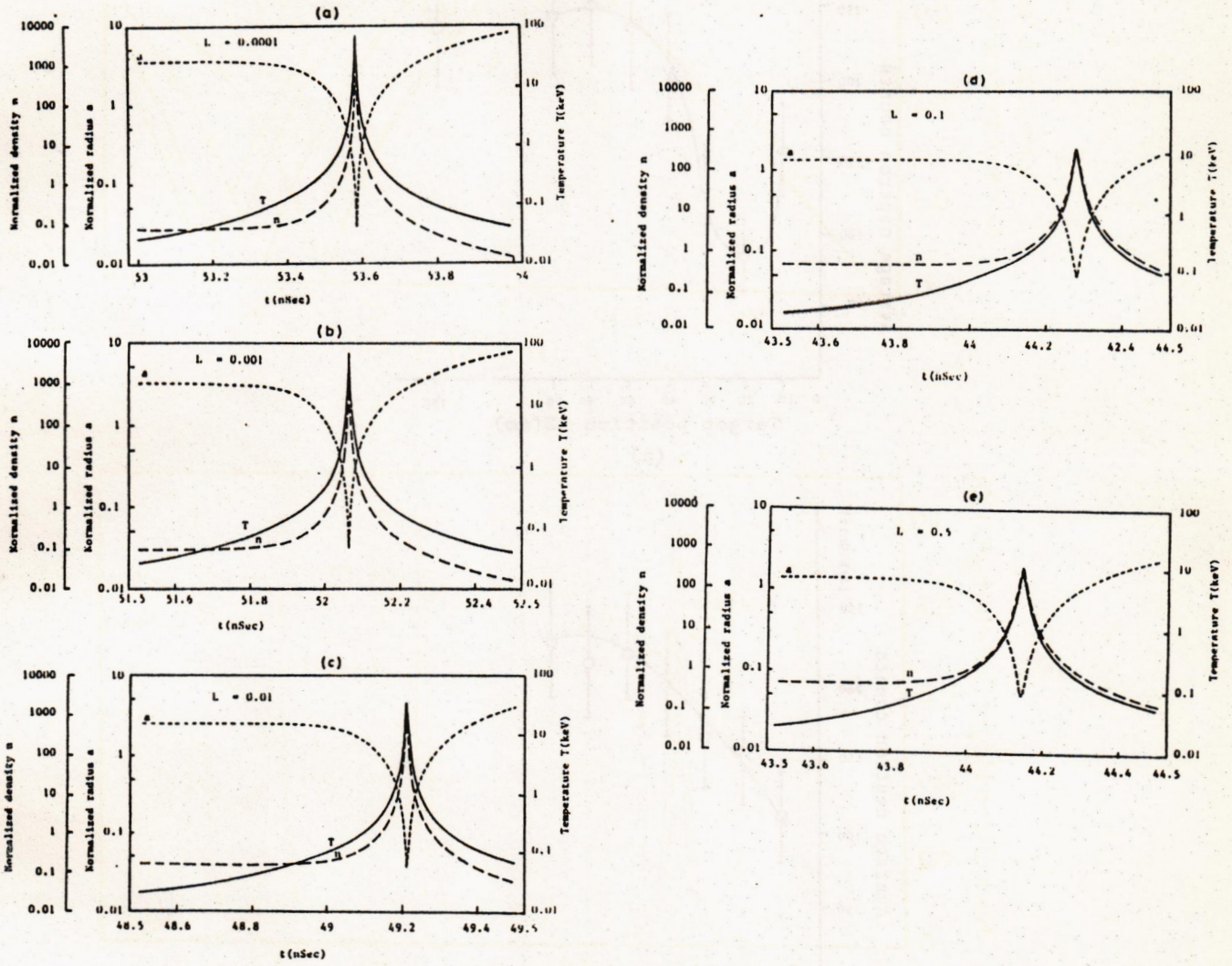

Figure 5: Plots of the normalized fiber plasma radius a, temperature T and density n for various gas-puff thicknesses L: a) $L = 0.0001$, b) $L = 0.001$, c) $L = 0.01$, d) $L = 0.1$, e) $L = 0.5$

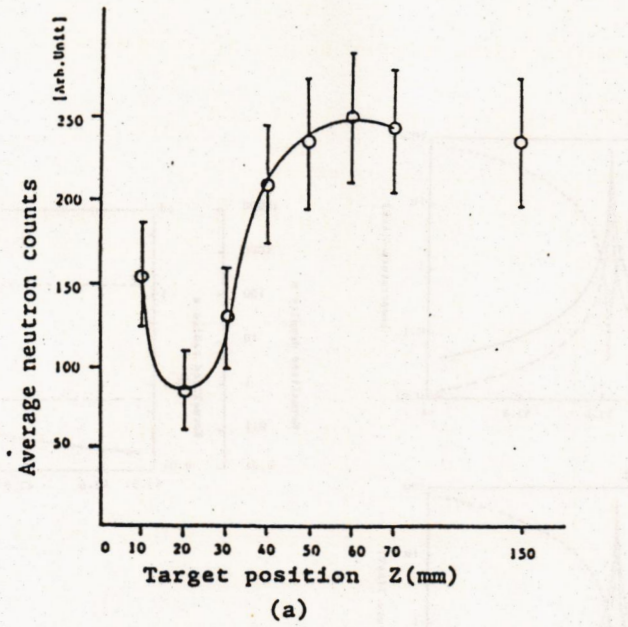

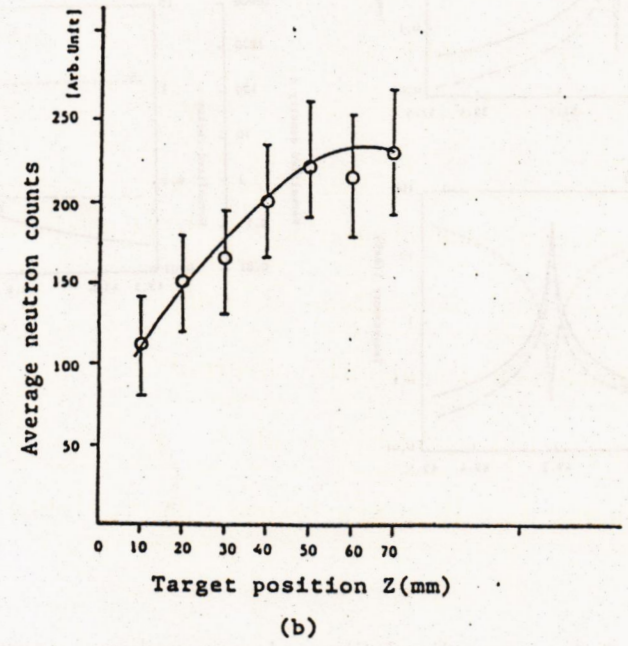

Figure 6: Average neutron yield as a function of target distance from the tip of the anode (a) without hole and (b) with a hole in the center of the target

Table 1: Value of the inverse bremsstrahlung term and the flux inhibition factor f for various laser wavelengths, intensities and temperatures at the critical surface for $Z = 4$, $T_H = 2T_c$, $n_H = n_c$ and $\ln \Lambda_{ee} = \ln \Lambda_{ei}$

$\lambda(\mu m)$	$I(10^{14} W/cm^2)$	$T_H(keV)$	$(1 + \tilde{\delta}_{IB}/T_c)$	f
1.06	3	2.3	1.07	0.163
1.06	6	2.8	1.116	0.17
0.353	4.5	1.7	1.016	0.155
0.353	10	2.4	1.025	0.156

Table 2: Flux inhibition factor f as proposed by different nonlocal models for $Z = 4$, $T_H = 2T_c$, $n_H = n_c$ and $\ln \Lambda_{ee} = \ln \Lambda_{ei}$

f	Model
0.51	Matte et al.-simulation results with inverse-bremsstrahlung effect.
0.21	Luciani et al.-nonlocal model result.
0.46	Albritton et al.-nonlocal model result.
0.15	Bendib et al.-simulation result.
0.15-0.17	Our results with inverse-bremsstrahlung absorption term.

References

[1] N.R.Pereira, N.Rostoker, J.Riodan, and M.Gersten in proceeding ofthe First International Conference on Dense Z-pinches for Fusion, edited by J.D. sethian and K.A.Berger (Navel Research Laboratory, Washington, D.C., (1984), p.71.

[2] J.E.Hammel, D.W.Scudder, and J.S. Schlachter, in [?],p.13.

[3] D.W.Scudder, Bull. Am. Phys. Soc. 30, 1408 (1985); D.W.Scudder, R.Y. Dagazian, J.E.Hammel and P.r. Forman, Bull. Am. Phys. Soc. 31, 2581(1986).

[4] "Enhanced stability and neutron production in a dense Z-pinch plasma formed from a frozen deutrium fiber". J.D. Sethian, A.E.Robson, K.A.Berger and A.W. DeSilva, Phys. Rev. Lett. 59, 892 (1987).

[5] "Fusion by a $Z-\theta$ pinch", H.U. Rahman, F.J. Wessel, A.Fisher and N.Rostoker, Bull. Am. Phys. Soc. 32, 1818 (1987).

[6] H.U. Rahman, P.Ney, F.J. Wessel, A.Fisher and N.Rostoker, AIP Conference Proceedings 195; Dense Z-pinches, New York, 1989, p.351.

[7] "Generation of high magnetic fields using a gas-puff Z-pinch", F.J.Wessel, F.S.Felber, N.C.Wild, H.U.Rahman. E.Ruden and A.Fisher, Appl. Phys. Lett. 48, 1119(1986).

[8] "Faraday rotation in a multimode optical fiber in a fast rise time, high magnetic field", F.J.Wessel, N.C.Wild, A.Fisher, H.U.Rahman and F.S.Felber, Rev. Sci. Instrum. 57, 2246(1986).

[9] N.A.Ratakhin, S.A.Sorokin, S.A.Chaikovsky, Proc. Seventh Int. Con. on High Power Particle Beams, Vol.II, 1204(1988).

[10] F.S.Felber, M.M.Malley, F.J.Wessel, M.K.Matzen, M.A.Palmer, R.B.Spielman, M.A.Liberman and A.L.Velikovich, Phys. Fluids, 31, 2053(1988).

[11] "Ultrahigh magnetic fields produced in a gas-puff Z-pinch", F.S.Felber, F.J.Wessel, N.C.Wild, H.U.Rahman, A.Fisher, C.M.Fowler, M.A.Liberman and A.L.Velikovich, J.Appl.Phys., 64, 3831(1988).

[12] "Theoretical model for a finite-thickness gas-puff $Z-\theta$ pinch", Arshad.M.Mirza, M.Iqbal, N.A.D.Khattak and G.Murtaza, Modern Phys. Lett. B, 7,1655(1993).

[13] "Fusion conditions in a finite-thickness gas-puff staged Z-pinch", Arshad.M.Mirza, N.A.D.Khattak, M.Iqbal and G.Murtaza, Journal of Plasma Phys. (in press)

[14] "Laser absorption and heat transport by non-Maxwellian-Boltzman electron distribution", J.R.Albritton, Phys. Rev. Lett., 50, 2087(1983).

[15] "Nonlinear inverse Bremsstrahlung and heated electron distributions", A.B.Langdon, Phys. Rev. Lett., 44, 575(1980).

[16] "Electron energy transport in steep temperature gradients in laser produced plasmas", A.R.Bell, R.G.Evans and J.Nicholas, Phys. Rev. Lett., 46, 243(1981).

[17] "Apparent and real thermal inhibition in laser produced plasmas", R.J.Mason, Phys. Rev. Lett., 47, 652(1981).

[18] "Heat transport formula in strongly inhomogeneous plasmas", A.M.Mirza, G.Murtaza and M.S.Qaisar, Phys. Lett. A., 141, 56(1989).

[19] "Nonlocal heat transport due to steep temperature gradients", J.F.Luciani, P.Mora and J.Virmont, Phys. Rev. Lett., 51, 1664(1983).

[20] "Role of inverse Bremsstrahlung absorption and electrostatic potential on energy transport mechanism in laser produced plasmas",G.Murtaza, Arshad.M.Mirza and M.S.Qaisar, Physica Scripta, 50,403(1993).

[21] J.P. Matte and J. Virmont, Phys. Rev. Lett. **49**, 1936 (1982).

[22] "Sequential focusing in Mather-type plasma focus", M.Nisar, F.Y.Khattak, G.Murtaza, M.Zakaullah and N.Rashid, Physica Scripta, 47, 814(1993).

Modern Physics Letters B, Vol. 7, No. 26 (1993) 1655–1660

THEORETICAL MODEL FOR A FINITE-THICKNESS GAS-PUFF Z–Θ PINCH

ARSHAD M. MIRZA, M. IQBAL, N. A. D. KHATTAK, and G. MURTAZA
Department of Physics, Quaid-i-Azam University, 45320 Islamabad, Pakistan

Received 27 January 1993
Revised 5 November 1993

A dynamic model for a finite-thickness gas-puff Z–θ pinch is proposed. The snowplow effect is incorporated to describe the dynamics of an imploding annular plasma shell of finite thickness. Our numerical results demonstrate that for a thick gas-puff layer, fast compression occurs which produces an ultrahigh magnetic field on a time scale much less than the rise time of the Z-pinch current. For a very thin puff layer, however, the current sheath moves like a constant mass layer as described by Rahman *et al.*

1. Introduction

The Z-pinch enjoys the simplest geometry and operational characteristics among all the proposed thermonuclear fusion devices to date. It consists of a radially imploding plasma confined by azimuthal self-magnetic field B_θ generated by an axial current I through the plasma.[1] Earlier work in the field of thermonuclear fusion research revolved around this simple geometry as its theoretical analysis was easy. However, it was soon discovered that the plasma in such a device becomes highly unstable due to MHD instabilities (namely the Sausage and Kink instabilities) as well as the end losses. To stabilize the Z-pinch plasma, various methods have been employed, such as the inclusion of an axial magnetic field B_z and conducting walls. Recent advances in high-voltage, high-current pulsed technology have helped in obtaining a plasma close to thermonuclear fusion conditions with the simple Z-pinch geometry (with an enhanced stability).

There are several uses of the Z-pinch device, e.g., it can produce ultrahigh magnetic fields (> 40 MG) through fast compression of initially weak fields by the imploding plasma.[2–4] It can also be used as X-ray source and is proposed as a potential device for X-ray lasers[5–7] which in turn can be used as a driver for ICF (Inertial Confinement Fusion). The Z-pinch device is also suitable for plasma diagnostic studies and spectroscopic measurements.

Felber *et al.*[10] proposed a novel method to produce a magnetic field of the order of 100 MG by executing fast compression of a magnetic flux with an imploding annular plasma liner. In this technique, an annular gas-puff Z-pinch compresses

the magnetic flux in the same way as a solid density conductor in an explosive flux compression generator. The Z-pinch method, which involves no explosive or material deformation, can be extrapolated to much higher fields than the conventional techniques and provides a higher repetition rate. The feasibility of this method has been checked in some recent experiments by Baksht *et al.*[11] and by Felber *et al.*[4,6] There is also some experimental evidence that magnetic field up to ~42 MG has been seen by using the PROTO-II pulsed-power generator.

Recently, some experiments on a Z-pinch have been performed by using solid fiber or cryogenic deuterium fiber.[12] Initially, the inductance of the fiber is large and consequently, the current rise time is $\sim$ 10 nsec. The fiber material heats up, evaporates and becomes a low density plasma. This plasma expands and continues to do so up to the time the magnetic pressure exceeds the kinetic pressure of the plasma. But the plasma soon becomes unstable without achieving high density. To circumvent this, a new hybrid scheme of Z–θ pinch has been proposed.[13] In this scheme, an annular Z-pinch plasma implodes an axial B_z-magnetic field compressing it to many megagauss with a current rise time of an order of magnitude shorter than the Z-current. At the axis of the Z-pinch, a solid fiber or straw is placed which breaks down and forms a θ-pinch. The current rise time of the θ-pinch is a few nsec and this Z–θ configuration is found to be much more stable than the ordinary Z-pinch configuration. Such Z–θ pinch machines are in operation in various laboratories including UC-Irvine, Sandia Laboratory, and in USSR.[2–4,6,14] The maximum axial field reported so far is of 40 MG (Sandia). The plasma produced in this way is found to be sufficiently hot and dense to become a useful neutron source.[15]

Rahman *et al.*[13] have proposed a model to study the dynamics of Z–θ pinch plasma with an entrained axial magnetic field B_z by considering an imploding annular plasma shell whose thickness is neglected. As the Z-pinch plasma implodes, it compresses the axial B_z field to a very high value with extremely fast rise time. This changing magnetic field induces an azimuthal surface current J_θ around the solid fiber which diffuses into the fiber and produces an extremely hot plasma. The fast rise of induced current heats up the plasma by ohmic as well as adiabatic compression on a time scale much shorter than the radiative loss time and eventually creates plasma close to fusion conditions.

Since in most of the experiments, the gas-puff has finite thickness, theoretical modeling for such a Z–θ pinch plasma is in order. If we consider a fully ionized plasma and a perfect conductor, the initial discharge current would flow on the outer surface of the plasma, parallel to the axis of the cylinder in the form of a current sheath which sets up an azimuthal magnetic field B_θ just outside the current layer. Since there is no field inside the gas-puff plasma, the sheath experiences an inward pressure $B_\theta^2/8\pi$ and so begins to contract. As it moves inward, the current sheath behaves like a magnetic piston and sweeps up all the plasma particles it encounters. This is the so-called snowplow model.[16] For a finite-thickness gas-puff, the snowplow effect would occur in the puffed region and when the outer current sheath reaches

the inner puffed region, it would move like a thin constant mass layer, as described by Rahman *et al.*

In this paper, we investigate a finite-thickness gas-puff using the snowplow model. Our results indicate that for thick gas-puff layer, the compression of the axial magnetic field occurs earlier than in the results of Rahman *et al.*[13]

2. Dynamic Model of Z-pinch with an Entrained Axial Magnetic Field

We consider a simple model for the dynamics of an imploding annular plasma shell of finite thickness. If at the initial instant, the gas-puff is located in a cylindrical shell $r_1 < r < r_0$, where r_0 is the inner radius of the discharge tube such that $(r_0 - r_1)$ is the gas-puff thickness L, then the inward velocity of the current sheath can be obtained by using the snowplow model which essentially balances the rate of change of momentum of the swept plasma with the magnetic pressure, i.e.

$$\frac{d}{dt}\left(M\frac{dr}{dt}\right) = -2\pi r P_{\text{mag}}\,, \tag{1}$$

where M is the mass per unit length of the plasma swept by the current sheath as it moves inward and P_{mag} is the net magnetic pressure on the Z–θ pinch.

The swept mass per unit length M is given by

$$M = \pi(r_0^2 - r^2)\rho_{\text{m}}\,, \tag{2}$$

where ρ_{m} is the initial mass density of the gas-puff.

The azimuthal magnetic field due to current I just outside the sheath of radius r is

$$B_\theta = \frac{\mu_0 I}{2\pi r}\,,$$

or, in C.G.S. units,

$$B_\theta = \frac{I(\text{amp})}{5r(\text{cm})}\,. \tag{3}$$

If the axial magnetic flux is conserved, the field at maximum compression ($r = r_{\text{m}}$) is given by

$$B_z = B_0\left(\frac{r_0}{r_{\text{m}}}\right)^2. \tag{4}$$

Therefore, the magnetic pressure P_z acting on the Z-pinch plasma due to B_z is

$$P_z = \frac{B_0^2}{8\pi}\left(\left(\frac{r_0}{r}\right)^4 - 1\right). \tag{5}$$

The total magnetic pressure P_{mag} accelerating the Z-pinch plasma is $B_0^2/8\pi - P_z$ and is given by

$$P_{\text{mag}} = \frac{1}{8\pi}\left(\left(\frac{I}{5r}\right)^2 + B_0{}^2\left(1 - \left(\frac{r_0}{r}\right)^4\right)\right). \tag{6}$$

It may be noted here that when r becomes minimum, P_z accelerates the plasma in the direction of increasing r.

Finally, Eqs. (1) and (6) give

$$\frac{d}{dt}\left(\pi(r_0^2 - r^2)\rho_m \frac{dr}{dt}\right) = -\frac{r}{4}\left(\left(\frac{I}{5r}\right)^2 + {B_0}^2\left(1 - \left(\frac{r_0}{r}\right)^4\right)\right). \tag{7}$$

Suppose that the discharge current rises according to a sine function profile as is approximately the case when the capacitor bank is switched into the circuit, i.e.

$$I = I_m \sin\left(\frac{\pi t}{2t_0}\right), \tag{8}$$

where t_0 is the current rise time and I_m the maximum current.

In the dimensionless form, the above equation becomes

$$\frac{d}{d\tau}\left((1 - R^2)\frac{dR}{d\tau}\right) = -\frac{a}{R}\left(\sin^2\left(\frac{\pi\tau}{2}\right) - \frac{b}{R^2}(1 - R^4)\right), \tag{9}$$

with $a = I_m^2 t_0^2/100mr_0^2$, $b = (5B_0r_0/I_m)^2$, $R = r/r_0$, $\tau = t/t_0$, and m defined as $\pi r_0^2\rho_m$ represents the mass per unit length of the plasma. It may be noted here that the above equation is valid only in the gas-puffed region where the snowplow effect occurs. When the current sheath reaches the inner puffed region, it would move like a thin current layer as described in Ref. 13.

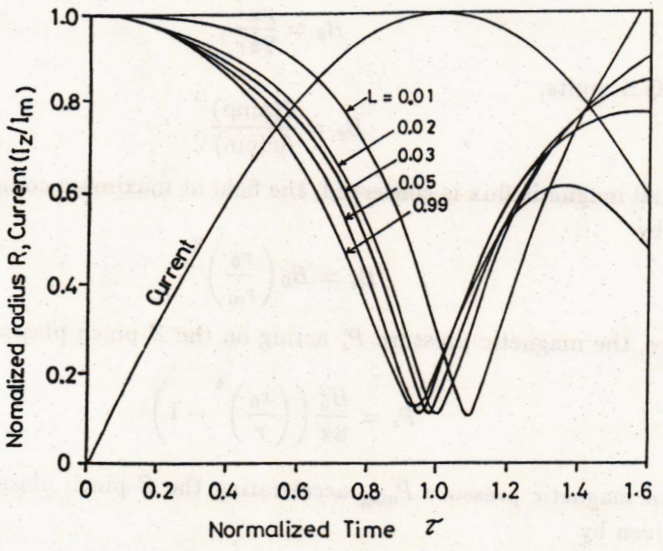

Fig. 1. Normalized characteristics of Z–θ pinch with entrained axial magnetic field for various puff thicknesses and for a sinosidal current profile.

Taking typical parameters of UCI experiments,[13] i.e. $I_m = 472$ kA, $B_0 = 10$ kG, $t_0 = 1$ μsec, $m = 10^{-4}$ g/cm, $b = 0.045$, and $a = 4$, we numerically simulate this problem for different values of the puff thickness L. Our results show that for a very thin puff layer ($L \sim 0.01 r_0$), the Rahman *et al.*[13] model works very well, i.e. one obtains maximum compression (corresponding to minimum radius $R \sim 0.1$) after a time of the order of 1.1 times the curent rise time. On the other hand, for puff thickness $0.01 < L/r_0 < 0.99$, we obtain the compression at an earlier time. In all cases, the compression time is an order of magnitude less than the current rise time. Figure 1 shows the variation of imploding plasma radius with time for various gas-puff thicknesses. For a very thick gas-puff $L \sim r_0$, the plasma sheath reaches maximum compression ($r \sim 0.1 r_0$) after a time 0.94τ. We have found that for puff thickness $L > 0.1 r_0$, all the R vs τ curves converge to the curve corresponding to time $0.94 t_0$. Figure 2 exhibits how the axial magnetic field varies in time for different values of the puff thickness. The snowplow effect evidently changes the timing of the fast compression. There may also be a stabilizing effect on the Rayleigh Taylor instability as discussed by Gol'berg and Velikovich.[17]

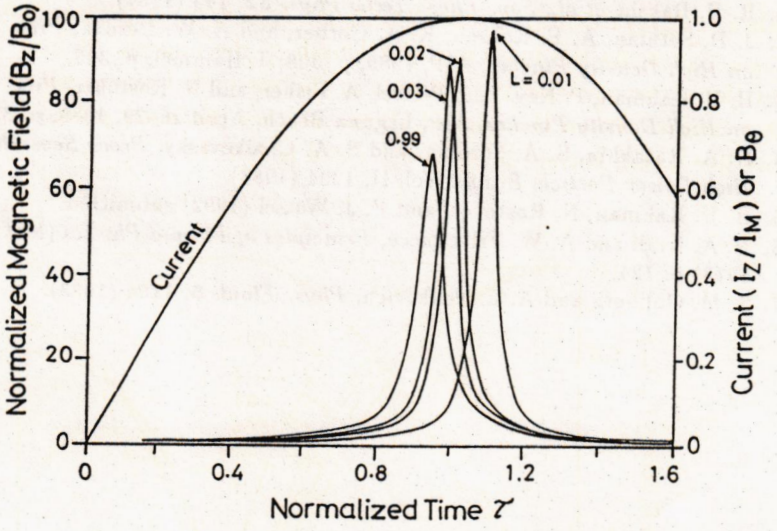

Fig. 2. Normalized magnetic field vs normalized time for various gas-puff thicknesses with sinosidal current profile.

Acknowledgements

One of us (A. M. Mirza) gratefully acknowledges fruitful discussions with Professor N. Rostoker during the 17th International Nathiagali Summer College on Physics and Contemporary Needs (1992) in Pakistan. We are also grateful to the referee for valuable suggestions and for pointing out some misprints in the paper which has indeed improved the quality of the work. This work is partially supported by the

World Laboratory CHEPCI Project, Pakistan, and the Pakistan Science Foundation Projects C-QU/Phys(69) & (75).

References

1. D. J. Rose and Clark, *Plasmas and Controlled Fusion* (MIT Press, 1961) Chap. 14.
2. F. J. Wessel, F. S. Felber, N. C. Wild, H. U. Rahman, A. Fisher, and E. Ruden, *Appl. Phys. Lett.* **48**, 1119 (1986).
3. F. J. Wessel, N. C. Wild, A. Fisher, H. U. Rahman, A. Ron, and F. S. Felber, *Rev. Sci. Instrum.* **57**, 2246 (1986).
4. F. S. Felber, M. M. Malley, F. J. Wessel, M. K. Matzen, M. A. Palmer, R. B. Spielman, M. A. Liberman, and A. L. Velikovich, *Phys. Fluids* **31**, 2053 (1988).
5. S. J. Stephanakis *et al.*, *IEEE Trans. Plasma Sci.* **16**, 472 (1988).
6. F. S. Felber, F. J. Wessel, N. C. Wild, H. U. Rahman, A. Fisher, C. M. Fowler, M. A. Liberman, and A. L. Velikovich, *J. Appl. Phys.* **64**, 3831 (1988).
7. J. Davis *et al.*, *IEEE Trans. Plasma Sci.* **16**, 472 (1988).
8. K. H. Finken and Ü. Ackerman, *Phys. Lett.* **A85**, 278 (1981).
9. K. H. Finken and Ü. Ackerman, *J. Phys.* **D16**, 773 (1983).
10. F. S. Felber, M. A. Lieberman, and A. L. Velikovich, *Appl. Phys. Lett.* **46**, 1042 (1985).
11. R. B. Baksht *et al.*, *Sov. Phys. Tech. Phys.* **32**, 145 (1987).
12. J. D. Sethian, A. E. Robson, K. A. Gerber, and A. W. Desilva, *Proc. 2nd Int. Conf. on High Density Pinches*, AIP, 1989, p. 308; J. Hammel, p. 303.
13. H. U. Rahman, P. Ney, F. J. Wessel, A. Fisher, and N. Rostoker, *Proc. 2nd Int. Conf. on High Density Pinches*, AIP, Laguna Beach, April 26–29, 1989, p. 351.
14. N. A. Ratakhin, S. A. Sorokin, and S. A. Chaikovasky, *Proc. Seventh Int. Conf. on High Power Particle Beams*, Vol. II, 1204 (1988).
15. H. U. Rahman, N. Rostoker, and F. J. Wessel (1992) submitted.
16. N. A. Krall and A. W. Trivelpiece, *Principles of Plasma Physics* (McGraw-Hill, N.Y., 1973) p. 124.
17. S. M. Gol'berg and A. L. Velikovich, *Phys. Fluids* **5**, 1164 (1993).

Fusion Conditions in a Finite-Thickness Gas-Puff Staged Z-Pinch

by

Arshad M. Mirza, N.A.D. Khattak, M. Iqbal and G. Murtaza
Department of Physics, Quaid-i-Azam University,
Islamabad 45320, **Pakistan**

Abstract

We investigate the implosion of a dense θ-pinch plasma driven by an annular finite-thickness gas-puff Z-pinch. The imploding Z-pinch traps an axial magnetic field B_Z compressing it to large values in an extremely short time. The temporal variation of B_Z then induces an azimuthal θ-current on the surface of a fiber placed on the axis with a rise time an order of magnitude shorter than the rise time of Z-pinch current. Our numerical results demonstrate that for a thick gas-puff layer, maximum compression occurs before the current peaks. We also find that at peak compression, fuel density of the order of $10^{25}/cm^3$ and temperature >10 keV can be achieved on a time scale of the order of 0.1 nsec. Thus the Lawson parameter $n\tau \sim 10^{14}$ sec/cm^3 for a D-T fiber becomes achievable. The Snowplow effect in the Z-pinch exercises a stabilization effect on the growth of Sausage and Rayleigh-Taylor instability. In the limits of a very thin gas-puff layer, previous results are fully recovered.

1. Introduction

Z-pinch was among the first approaches to fusion because of its simplicity. Early Z-pinch devices relied on the implosion of a low-density plasma onto the axis of a cylindrical chamber. They were, however, found to be violently unstable due to sausage (m=0) and kink (m=1) instabilities. To stabilize the Z-pinch plasma, various methods were employed such as the inclusion of an axial magnetic field B_z or conducting walls. However, recent experiments using a novel technique of pinch formation have produced pinches that appear to be stable for much longer time than expected on the basis of ideal MHD theory (Sethian *et al.* 1987; Hammel *et al.* 1987). These pinches are formed from frozen deuterium fiber on which the currents rise very rapidly when very high voltages are applied. The pinch shows stability as long as the current is rising but succumbs to a rapidly growing m=0 instability when the current saturates. This phenomenon is independent of the magnitude of the current and other pinch parameters (Sethian *et al.* 1991).

In 1985, Felber *et al.*, suggested a method of producing a magnetic field of the order of 100 MG. This method involves fast compression of magnetic flux by an imploding annular plasma liner which compresses the magnetic flux in the same way as a solid density conductor does in an explosive flux compression generator. This method, which involves no explosive or material deformation, can be employed to produce fields much higher than the conventional techniques and a higher repetition rate. The feasibility of this method has been demonstrated in some recent experiments (Baksht *et al.* 1987; Felber *et al.* 1988). There is also some experimental evidence that magnetic field up to 40 MG has been seen by using the PROTO-II pulsed power generator.

Recently, a new scheme known as a staged pinch or Z-θ pinch has been proposed (Rahman *et al.* 1989). In this hybrid scheme an annular Z-pinch plasma implodes onto an axial B_Z magnetic field compressing it to multi-megagauss fields with a rise time at least an order of magnitude shorter than that of the Z-current. The rapidly rising B_Z field, in the presence of radiation from the imploding Z-pinch, induces a θ -pinch discharge on the surface of the co-axial structure converting it to a dense high temperature plasma. The current rise time of θ-pinch is few nanoseconds and this Z-θ configuration is found to be more stable than the ordinary Z-pinch (Spielman *et al.* 1985; Rahman *et al.* 1989). Such staged pinch devices are now in operation in various laboratories including UC-Irvine (Wessel *et al.* 1986), Sandia Laboratory (Felber *et al.* 1988) and in USSR (Ratakhin *et al.* 1988). The measured axial fields are 1.6 MG (UCI), 2.5 MG (USSR) and 40 MG (Sandia).

The dynamics of Z-θ pinch plasma with an entrained axial magnetic field B_Z has been considered by Rahman *et al.* (1989), assuming a very thin imploding annular plasma shell. As the Z-pinch implodes, the highly conductive plasma traps the axial magnetic field B_Z compressing it to megagauss levels with extremely fast rise time. The rapidly rising B_Z field then induces a θ-pinch discharge on the surface of the coaxial structure converting it to a dense high temperature plasma. The fast rise of induced current heats up the plasma by Ohmic heating as well as by adiabatic compression on a time scale much shorter than the radiative loss time and eventually creates plasma close to fusion conditions. Apart from fusion, the staged pinch has applications in photo-resonant and recombination x-ray lasers (Apruzes *et al.* 1989; Stephanakis *et al.* 1988,) which in turn can be used as a driver for Inertial Confinement Fusion (ICF).

To simulate the actual experimental conditions, the outer gas-puff must have some finite thickness. Theoretical modeling for a Z-θ pinch with a finite thickness is therefore very much in order. We have already investigated the said effect (Mirza *et al.* 1993) in the context of a Z-pinch plasma using the well known Snowplow model. It may be noted that for a finite thickness gas-puff, the Snowplow action is effective only as long as the current sheath remains inside the puff region. Once the current sheath reaches the puff boundary, it then moves on like a thin constant mass layer as described in Rahman *et al.*(1989) model. Our ivestigation has demonstrated that a thick gas-puff layer causes compression of the axial magnetic field faster than a thin-puff layer.

In this paper, we study the Z-Θ pinch and investigate how a finite-thickness gas-puff would effect its dynamics. Our numerical results indicate that for a thick gas-puff layer, fast compression occurs producing an ultrahigh magnetic field (~100 MG) on a time scale much faster than the rise time of the Z-pinch current. We also find that at the peak compression, fuel density ~10^{25}/cm^3 and temperature > 10 keV can be achieved in as short a time as 0.1 nsec and thus the Lawson parameter nτ ~ 10^{14} sec/cm^3 can easily be achieved. This demonstrates the efficacy of a staged pinch as a good candidate for controlled thermonuclear fusion device.

2. Dynamic Model for a Staged Pinch

We first consider the dynamics of the outer Z-pinch plasma which is in the form of a cylindrical shell having some finite thickness. The dynamical equation for such a Z-pinch plasma based on Snowplow model is given by (Mirza *et al.*1993),

$$\frac{d}{dt}\left((1-R^2)\frac{dR}{dt}\right) = -\frac{I_m^{\,2}}{100mR\,r_0^{\,2}}\ \mathrm{Sin}^2\left(\frac{\pi t}{2t_0}\right) - \frac{B_0^{\,2}\,R}{4m}\left(1-\frac{1}{R^4}\right) \qquad (1)$$

where $R = r/r_0$ defines the normalized outer radius of the sheath annulus, t_0 is the quarter-period rise-time of the current in nsec, m defined as $\pi r_0^2 \rho_m$ (ρ_m being the mass density) represents the mass per unit length of the plasma in μgm/cm, I_m is the maximum current in MA and B_0 is the initial value of the applied axial magnetic field expressed in MG.

We have numerically solved the above nonlinear differential equation for the following initial conditions i.e., $I_m = 10$ MA, $B_0 = 0.02$ MG, $t_0 = 50$ nsec, $r_0 = 4$ cm and $m = 38$ μgm/cm. Fig. 1 shows the temporal variation of the imploding plasma radius and the magnetic field B_Z for different values of the gas-puff thickness. We observe that, as thickness increases the implosion becomes faster and thus the maximum plasma compression occurs earlier in time. The magnetic field shows a downward trend, the maximum value being about 100 MG for a very thin gas puff. We also note that the rise of $B_Z(t)$ is about 100 time faster than the Z-current. This rapidly changing B_Z field would then induce a J_0 current on the surface of the fiber and initiate a θ-Pinch.

To study the dynamics of the inner θ-pinch, we assume a uniform column of high density plasma, avoiding the computational problem of cold-start effect. Using momentum conservation with adiabatic conditions, we obtain the equation of motion

$$\frac{d^2a}{dt^2} = -\frac{200\, B_0^2}{n_0\, a_0^2}\left(\frac{a}{R^4} - 800\left(\frac{n_0\, T_0}{B_0^2}\right)\frac{T}{a} + a\left(1-\frac{1}{a^4}\right)\right) \qquad (2)$$

and the energy equation

$$\frac{dT}{dt} = -2(\gamma - 1)\,\frac{T}{a}\frac{da}{dt} + \frac{(\gamma - 1)\, 10^{-22} q^2}{2 T_0\, n_0}(P_{ohm} - P_{rad}) \qquad (3)$$

where the radius a and temperature T of the fiber are normalized to their respective initial values a_0 , T_0 ; n_0 being the initial number density of DT-fiber plasma in the units

of $10^{22}/cm^3$. The Ohmic heating term P_{ohm} using the classical Spitzer resistivity $\eta_\perp$ (Book, 1990) is

$$P_{ohm} = \eta_\perp J_0^2$$

$$= 1.15 \times 10^{-14}\ Z\ ln\Lambda\ T^{-3/2}(kev)\ J_0^2$$

$$= 1.29 \times 10^{21} \left(\frac{B_0^2(MG)}{a_0^2(\mu m) T_0^{3/2}(keV)} \right) \frac{1}{a^2 T^{3/2} R^4} \qquad keV/nsec\text{-}cm^3$$

The main radiation losses P_{rad} included in our calculations are the bremsstrahlung and cyclotron power losses (Book, 1990) given by

$$P_{rad} = P_{br} + P_{cy}$$

$$= 3.32 \times 10^{20} \frac{n_0^2 (T\ T_0(keV))^{1/2}}{a^4} + 3.88 \times 10^{16} \frac{B_0^2(MG) n_0 T\ T_0(keV)}{a^2 R^4} \qquad keV/nsec\text{-}cm^3$$

The above three coupled nonlinear differential equations (1), (2) and (3) were solved numerically with initial values of $T_0 = 0.02$ keV, $B_0 = 0.02$ MG, $a_0 = 0.02$ cm and initial density n_0 of the order of $10^{22}/cm^3$. Fig. 1 depicts the normalized Z-current, outer radius R and the compressed magnetic field B_Z as a function of time for various values of the gas-puff thickness L normalized with r_0. We find that the maximum compression for a thick gas-puff occurs earlier in time than for a thin gas puff. The Snowplow effect also changes the timing of compression. A magnetic field with such a fast rise time would initiate θ-pinch on the surface of the coaxial fiber. In Fig. 2 we display the results for the inner θ-pinch D-T plasma i.e., the temporal variation of the plasma radius a, the density n and the temperature T for various puff thicknesses. Here we take into account Ohmic and adiabatic heatings and cyclotron and bremsstrahlung radiation losses. We observe that for very thin-puff layers (L-0.0001) , the earlier results of Rahman *et al.* (1989) are completely recovered i.e.

maximum compression takes place at 53.6 nsec. with $n \sim 5 \times 10^{25}/cm^3$ and T~70 keV. Note that the current rise time t_0 is 50 nsec. and thus the maximum compression for a very thin puff layer occurs after the current peaks. On the other hand, for relatively thick puff layer L~0.01, the maximum compression values of $n \sim 1.5 \times 10^{25}/cm^3$ and T~30 keV are achieved earlier than the current rise time. It is also evident from the graphs that for thick gas-puffs $L \geq 0.1$, the curves for R, a, n and T converge to the same curve corresponding to the time around 44.2 nsec thus obviating the necessity of increasing L beyond 0.1 .

It has been observed experimentally (Edison *et al.*1993) that the Z-pinch plasma transfers its energy to the fiber at the time when the compression peaks. However, earlier model of thin-shell gas-puff (Rahman *et al.* 1989) has shown that the imploding Z-pinch plasma approaches the minimum radius after the current peaks (i.e., when $dI/dt=0$) and is believed to become highly unstable due to sausage instability (Sethian *et al.* 1987), destroying the uniformity of the plasma column before the transfer of energy completes. In our model, on the other hand, the compression occurs before the current peaks and that might explain the stable pinch formation in our case.

The Snowplow effect which we have incorporated in the Z-pinch dynamics also provides an additional stabilizing factor (Gol'berg *et al.* 1993). In the acceleration phase of the outer Z-pinch plasma, the Rayleigh-Taylor instability is expected to occur which grows like $\xi=\xi_0 \exp(\gamma t)$ where $\gamma=(Kg)^{1/2}$ is the growth rate of instability, K is the wave number of the perturbation and $g=B_Z^2/8\pi m$, m being the mass per unit area of the Z-pinch. Since $S=gt^2/2$, one may obtain $\xi=\xi_0 \exp(2SK)^{1/2}$, where S is the distance to which the Z-pinch is accelerated. The instability can be controlled by minimizing the values of the initial perturbation ξ_0, the distance S to which the Z-

pinch is accelerated and the wave number $K = 2\pi/\ell$, where ℓ is the shell thickness which increases due to the Snowplow effect. Thus a thick shell Z-pinch plasma is expected to be more stable than a thinner one.

We thus conclude that thin gas-puff Z-θ pinches would be highly unstable against Sausage and Rayleigh-Taylor instability and might not be useful for controlled thermonuclear fusion devices. However, relatively thick gas-puff Z-θ pinches might prevent that circumstance. For example for L ~ 0.01, we find that $n \sim 10^{25}/cm^3$ can be achieved on a time scale of the order of 0.1 nsec which corresponds to the Lawson parameter $n\tau \sim 10^{14}$ sec/cm^3.

Acknowledgments

The authors are thankful to Dr. H. U. Rahman for fruitful discussions.
This work is partially supported by the Pakistan Science Foundation Project **C-QU/Phys(69)** and the Pakistan Atomic Energy Commission Project.

REFERENCES

Apruzese, J. P. & Davis, J. 1989 *Proc. Int. Conference on Lasers '89*, Dec. 3 - 8, 1989, p.7.

Baksht, *et al.* 1987 *Sov. Phy. -Tech. Phy.*, **32**, 145.

Book, David L., 1990, NRL Plasma Formulary, Naval Research Laboratory publication 0084-4040, Washington D.C.

Edison, N.S., Etlicher, B., Chuvatin, A.S., Attelan, S. & Aliaga, R. 1993 *Phys. Rev. E.* **48**, 3893.

Felber, F.S., Wessel, F.J., Wild, N.C., Rahman, H.U., Fisher, A., Fowler, C. M., Liberman, M. A. & Velikovich, A.L. 1988 *J. App. Phy.*, **64**, 3831.

Felber, F.S., Malley, M.M., Wessel, F.J., Matzen, M.K., Palmer,M.A., Spielman, R.B., Liberman, M.A. & Velikovich, A.L. 1988 *Phys. Fluids*, **31**, 2053.

Felber, F.S., Liberman, M.A. & Velikovich, A.L. 1985 *Appl. Phys. Lett.* **46**, 1042.

Gol'berg, S.M. & Velikovich, A.L. 1993 *Phys. Fluids*, **B5**, 1164.

Hammel, J.E. & Scudder, D.W 1987 *Proc. of 14th. European Conference on Cont. Fusion & Plasma Physics, Madrid* (EPS, Petit-lancy, Switzerland),pt.**2**, p.450.

Mirza, A. M., Iqbal M., Khattak, N.A.D. & Murtaza, G. 1993 *Mod. Phys. Lett.***B7**, 1655.

Rahman, H.U., Ney, P., Wessel, F.J., Fisher, A. & Rostoker, N. 1989 *Proc. 2nd Int. Conf. on Dense Z-Pinches, AIP, Laguna Beach*, April 26-29, p.**351**.

Ratakhin, N.A., Sorokin, S.A. & Chakovsky, S.A. 1988 *Proc. 7th. Int. Conf. on High Power Particle Beams*, Vol. **II**, 1204.

Sethian, J.D., Robson, A.E., Gerber, K.A. & DeSilva, A.W. 1987 *Phys.Rev. Lett.* **59**, 892.

Sethian, J.D. & Robson, A.E. 1991 *J. Fusion Energy*,**10**, 329.

Spielman, R.B., Matzan, M.K., Palmer, M.A., Rand, P.B., Hussey, T.W. & McDeniel, D.H. 1985 *Appl. Phys. Lett.* **47**, 229.

Stephanakis, *et al.*1988 *IEEE Trans. Plasma Sci.*, **16**, 472.

Wessel, F.J., Wild, N.C., Fisher, A., Rahman, H.U., Ron, A.& Felber,F. S. 1986 *Rev. Sci. Instr.*, **57**, 2247.

Fig.1. Normalized characteristics of the outer Z-pinch a) Plots of the outer radius R for various puff-thicknesses L and normalized axial current I_Z and b) compressed magnetic field B_Z (divided by 5000) for different L.

Fig.2. Plots of the normalized inner fiber plasma radius a, temperature T and density n for various gas-puff thicknesses L: a) L=0.0001, b) L=0.001, c) L=0.01, d) L=0.1, e) L=0.5

(a)

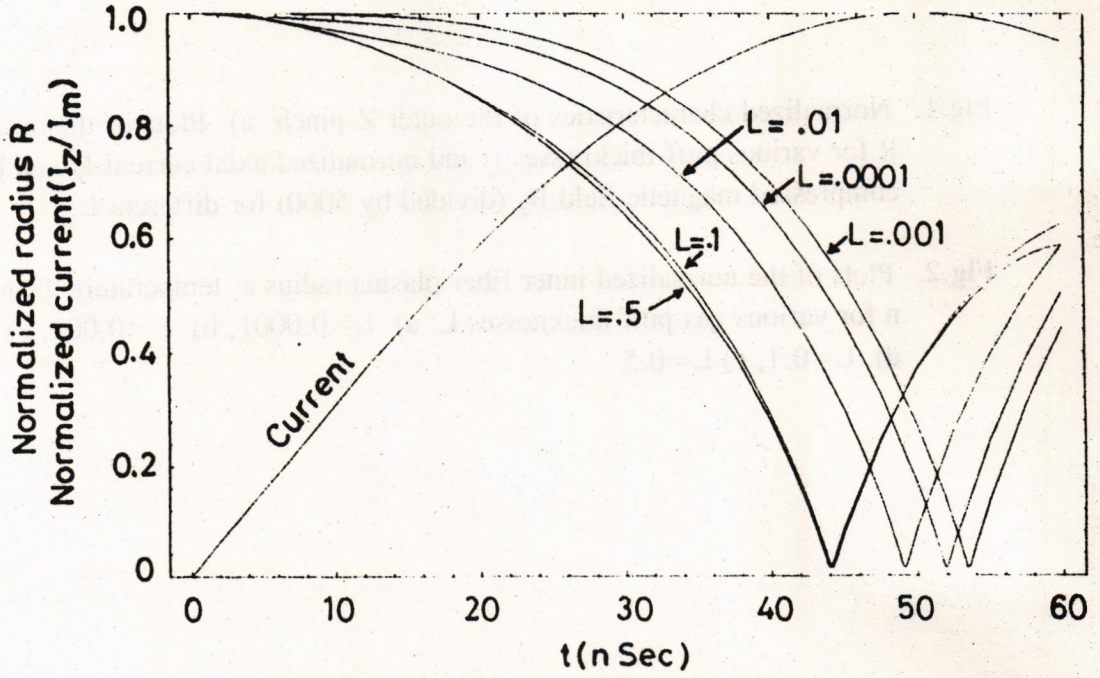
Normalized radius R
Normalized current(I_z/I_m)
1.0
0.8
0.6
0.4
0.2
0
0
10
20
30
40
50
60
t(n Sec)
L= .01
L=.0001
L=.001
L=.1
L=.5
Current

(b)

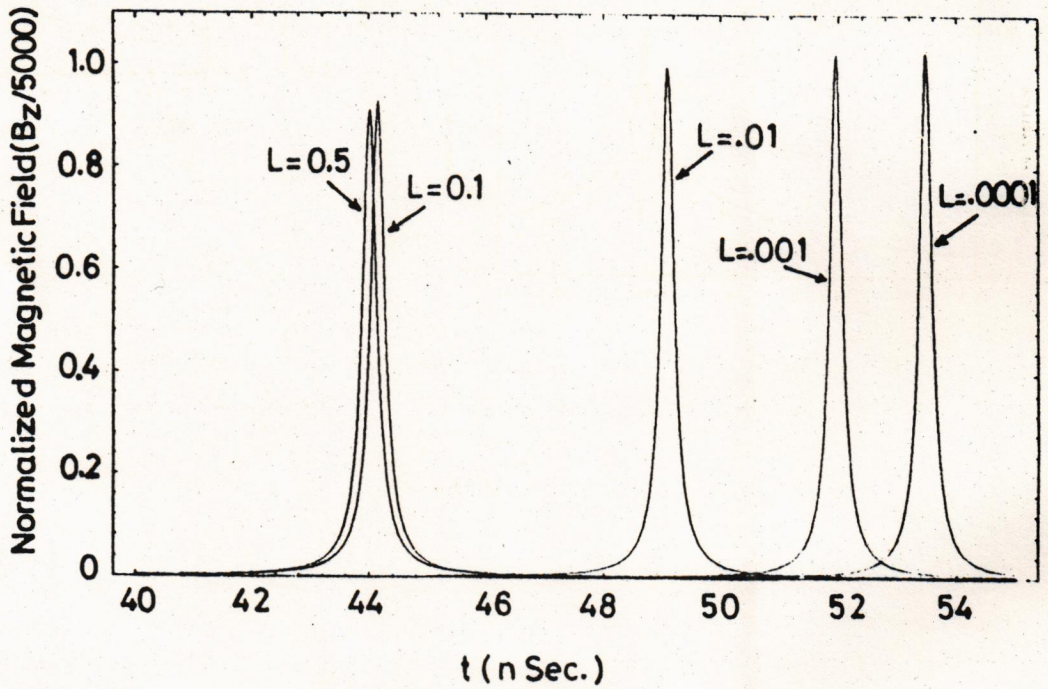
Normalized Magnetic Field(B_z/5000)
1.0
0.8
0.6
0.4
0.2
0
40
42
44
46
48
50
52
54
t (n Sec.)
L=0.5
L=0.1
L=.01
L=.001
L=.0001

Fig. 1

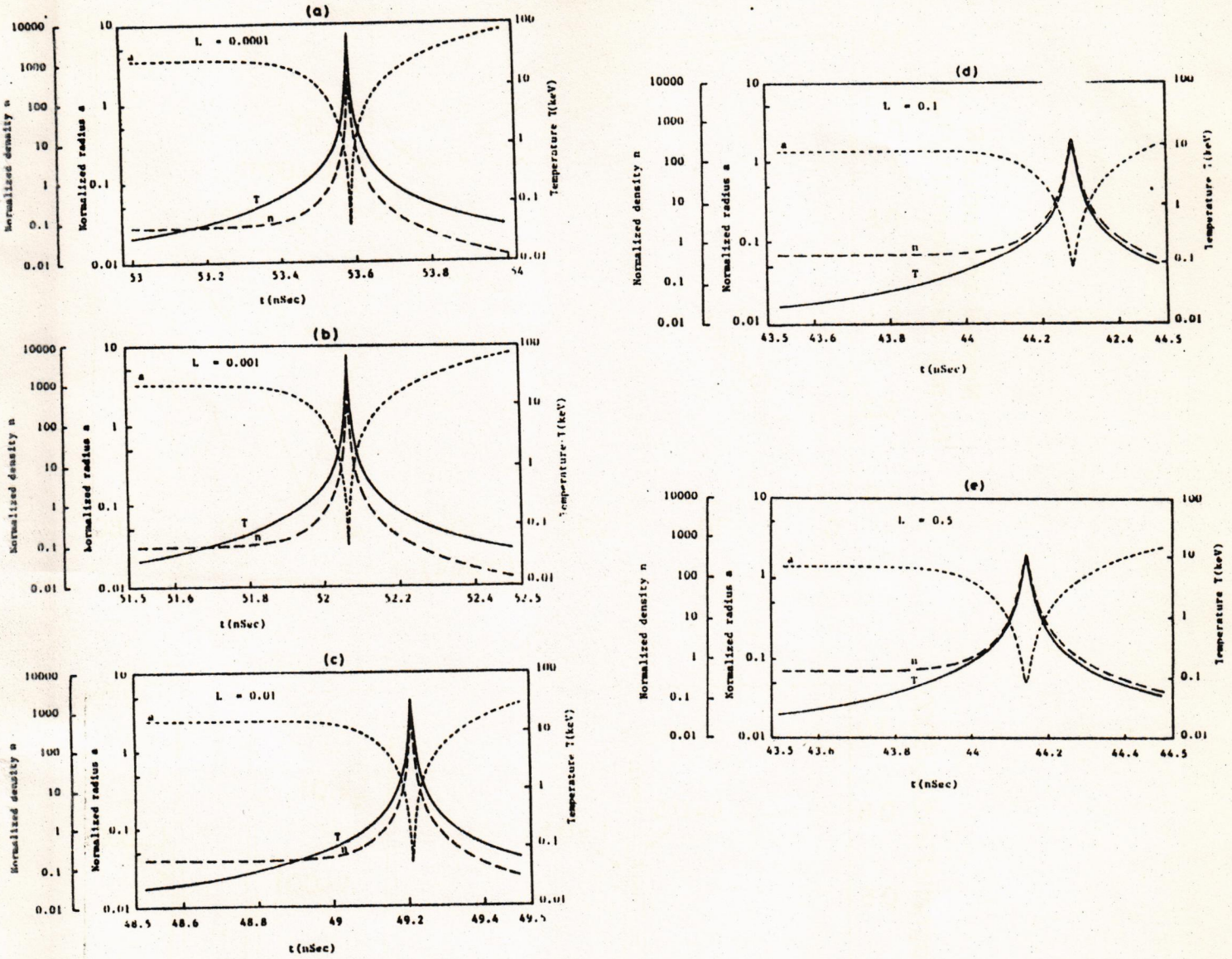
(a)
L = 0.0001
(b)
L = 0.001
(c)
L = 0.01
(d)
L = 0.1
(e)
L = 0.5
Normalized density n
Normalized radius a
Temperature T(keV)
t(nSec)
n
T
a

Fig. 2.

Physica Scripta. Vol. 50, 403–405, 1994

Role of Inverse Bremsstrahlung Absorption and Electrostatic Potential on Energy Transport Mechanism in Laser Produced Plasmas

G. Murtaza, Arshad M. Mirza and M. S. Qaisar

Department of Physics, Quaid-i-Azam University, 45320 Islamabad, Pakistan

Received February 18, 1994; accepted March 24, 1994

Abstract

An analytical nonlocal heat transport formula has been derived from the reduced Fokker-Planck equation for a strongly inhomogeneous laser produced plasma including inverse-bremsstrahlung absorption as well as the electrostatic potential. It is found that while the former contributes an additive term to the heat flux, enhancing its value for both steep- and gentle-gradient situations, the latter effect introduces an exponential term which significantly reduces the electron thermal transport. Our calculations also show that for a moderately intense laser field, the maximum heat flux for steep gradients situations corresponds to flux inhibition factor $f \sim 0.15$–0.17.

1. Introduction

The success of laser-induced fusion through compression of a spherical tiny target to super-high density depends upon laser energy absorption in the underdense region and then its efficient transfer from the lower density corona to a higher density ablation surface. It is important to directly heat as many electron as possible, but at the same time avoid generation of suprathermal electrons which can penetrate the core of the target before the final compression occurs.

Since in laser fusion, the laser energy is continuously being deposited at the top of the heat front and absorbed by the thermal electrons, a self-consistent treatment of the absorption process and the heat transport is in order. The most effective absorption mechanism for high-Z plasmas is the collisional inverse-bremsstrahlung process. This process leads to a slight overestimation of the absorption and of the transport itself. Albritton [1], used a simplified high-Z diffusion approximation of the Fokker-Planck equation to study the heat transport in laser produced plasmas and the Langdon [2] effect was taken into account to simulate the inverse-bremsstrahlung absorption process. Later on, Matte *et al.* [3] numerically simulated the laser plasma interaction with Fokker-Planck code, including the inverse-bremsstrahlung absorption as well as the ion-motion. The results were compared with the hydrocode LILAC, with adjustable flux limiter, f. The heat front was best modeled with flux limiting factor $f \sim 0.08$, in which case the coronal temperature was too high. The coronal temperature and density profile agree with $f = 0.15$.

There is a general concensus that the problem of heat transport under steep gradients produced by intense laser beam becomes nonlocal [4, 5] and that the isotropic part of the distribution function, f_0, cannot be taken to be a local Maxwellian. Attempts have been made to study the steep gradient situations by numerically solving the kinetic Fokker-Planck equation including electron-electron, electron-ion, and inverse-bremsstrahlung absorption term. But this approach seems to be very time-consuming and therefore, in most of the hydrodynamics codes, one generally uses simplified numerically efficient nonlocal models. In addition a number of analytical models based on the solution of kinetic Fokker-Planck equation have been proposed [6–11]. For example, Luciani *et al.* [7] and Albritton *et al.* [8] investigated how the electrostatic potential effects the nonlocal heat transport. Their conclusion was that the heat flux does not appreciably change. However, these models were found to be inadequate since the delocalization kernels had been assumed to remain unchanged by the electrostatic potential term. As Bendib *et al.* [9] pointed out that in the corona of a laser produced plasma a strong ambipolar field may exist that would prevent the fast moving electrons from escaping towards the vacuum. They also proposed a simple phenomenological nonlocal heat transport formula that gave good agreement with numerical simulations of the Fokker-Planck equation. Later, the effect of electrostatic potential on nonlocal heat transport was studied by Mirza *et al.* [11] by solving the reduced Fokker-Planck equation but ignoring the inverse-bremsstrahlung absorption term. On the other hand, Luciani and Mora [6] have proposed a nonlocal heat transport model which incorporated the inverse-bremsstrahlung absorption effect but did not include self-consistently the electrostatic potential effect.

We, in this paper, extend the previous nonlocal model [11] by solving the reduced Fokker-Planck equation and by including the local inverse-bremsstrahlung absorption. We systematically investigate its effect on nonlocal heat transport. The limiting cases for steep and gentle gradients are found to be modified and the ensuing results show good agreement with simulations of the kinetic Fokker-Planck equation possessing the inverse-bremsstrahlung absorption term.

2. Formulation of the problem

We start with the following set of Fokker-Planck equations in the diffusion approximation with an inverse-bremsstrahlung absorption term of Langdon [2]. Here we are not considering the case of strong anisotropy or intense laser field ($I > 10^{14}$ W/cm^2) since such a case may lead to

nonlinear absorption process (see e.g. [12]),

$$\frac{\partial f_0}{\partial t} + \frac{v}{3}\left[\frac{\partial}{\partial x} - \frac{eE}{mv}\left(\frac{\partial}{\partial v} + \frac{2}{v}\right)\right] f_1 = \frac{2v^2}{\lambda_\varepsilon}\frac{\partial}{\partial v}\left(\frac{T}{mv}\frac{\partial f_0}{\partial v} + f_0\right) + \frac{v^2 v_0^2 Z}{3(Z+1)\lambda_{90}}\frac{\partial}{\partial v}\left(\frac{1}{v}\frac{\partial f_0}{\partial v}\right), \quad (1)$$

$$\frac{\partial f_1}{\partial t} + v\left(\frac{\partial}{\partial x} - \frac{eE}{mv}\frac{\partial}{\partial v}\right) f_0 = \frac{2v^2}{\lambda_\varepsilon}\frac{\partial}{\partial v}\left(\frac{T}{mv}\frac{\partial f_1}{\partial v} + f_1\right) - \frac{2v}{\lambda_{90}} f_1, \quad (2)$$

where λ_ε is the energy loss mean-free-path, $\lambda_{90} = (mv^2)^2/2\pi ne^4(Z \ln \Lambda_{ei} + \ln \Lambda_{ee})$ (see e.g. [8]), v_0 is the electron quiver velocity, Z is the ionic charge state and f_0 and f_1 are the isotropic and anisotropic components of the electron distribution function respectively. It is worth mentioning here that the above two equations have been solved by Albritton *et al.* [8] and by Mirza *et al.* [11] for a high-Z plasma under static conditions, and with no inverse-bremsstrahlung absorption term. Also one can relate the electron quiver velocity, v_0, with the thermal velocity, v_{th}, in the high frequency laser field of intensity I and wavelength λ [13] as,

$$(v_0/v_{th})^2 \simeq 1.81 \cdot 10^{-16} I(\mathrm{W/cm^2})\lambda^2(\mu\mathrm{m})/T_e(\mathrm{keV}) \quad (3)$$

with $v_{th} = (T_e/m)$.

Transforming the independent variables from (x, v, t) to (x, ε, t), where $\varepsilon = mv^2/2 - e\phi(x, t)$, and assuming slow temporal variation for the distribution function as well as the potential ϕ (Kishimoto *et al.* [10] and Mirza *et al.* [11], eqs. (1) and (2) become,

$$\frac{\partial f_0}{\partial x} = -\frac{2}{\lambda_{90}} f_1, \quad (4)$$

$$\frac{\partial}{\partial x}[(\varepsilon + e\phi) f_1] = \frac{3(mv^2)^2}{\lambda_\varepsilon}\frac{\partial}{\partial \varepsilon}(f_0 - f_{MB}) + \frac{(mv^2)^2 mv_0^2 Z}{2(Z+1)\lambda_{90}}\frac{\partial^2 f_0}{\partial \varepsilon^2}. \quad (5)$$

Here we assume a high-Z plasma and approximate the parallel diffusion term with local Maxwell-Boltzmann distribution function $f_{MB} = n(m/2\pi T)^{3/2} \exp[-(\varepsilon + e\phi)/T]$ in eq. (5). If we assume that the heating term is not too strong then the inverse-bremsstrahlung source term takes a very simple form [3] by taking $f_0 = f_{MB}$. Then eqs (4) and (5) give,

$$\frac{\partial}{\partial \xi}\left[(\varepsilon + e\phi)^3 \frac{\partial f_0}{\partial \xi}\right] + \frac{\partial f_0}{\partial \varepsilon} = -\left(1 + \frac{\tilde{\delta}_{IB}}{T}\right)\frac{f_{MB}(\varepsilon, \xi)}{T(\xi)}, \quad (6)$$

where $\xi = x/\tilde{\lambda}_s$, $\tilde{\lambda}_s = (2\tilde{\lambda}_{90}\tilde{\lambda}_\varepsilon/3)^{1/2}$, $\tilde{\lambda} = \lambda/4(\varepsilon + e\phi)^2$ and $\tilde{\delta}_{IB} = mv_0^2 Z\lambda_\varepsilon/6(Z+1)\lambda_{90}$.

Equation (3) can also be rewritten as

$$\frac{\tilde{\delta}_{IB}}{T} \simeq 6 \cdot 10^{-9} ZI(10^{14}\,\mathrm{W/cm^2})\lambda^2(\mu\mathrm{m})/T_e(\mathrm{keV}). \quad (7)$$

Here we have taken $\ln \Lambda_{ee} = \ln \Lambda_{ei}$.

Notice that the eq. (6) has been solved by Albritton *et al.* [8] under the assumption $\varepsilon > e\phi$ and by Mirza *et al.* [11] by assuming that the potential ϕ is slowly varying and by ignoring the inverse-bremsstrahlung absorption term, $\tilde{\delta}_{IB}$. Here we retain the said term and solve eq. (6) by using the WKB physical optics approximation and obtain

$$f_0 = \int d\xi' \int_{\varepsilon + e\phi(\xi)} d\varepsilon' \times \frac{\exp[-(\xi - \xi')^2/\{(\varepsilon' + e\phi(\xi))^4 - (\varepsilon + e\phi(\xi))^4\}]}{\sqrt{\pi\{(\varepsilon' + e\phi(\xi))^4 - (\varepsilon + e\phi(\xi))^4\}}} \times (1 + \tilde{\delta}_{IB}/T)\frac{f_{MB}(\varepsilon', \xi')}{T(\xi')}. \quad (8)$$

The particle and heat fluxes are defined as

$$\{\Gamma, Q\} = -16\pi \int_{-e\phi}^{\infty} d\varepsilon\{1, (\varepsilon + e\phi(\xi))\} \times (\varepsilon + e\phi(\xi))^3 \frac{\tilde{\lambda}_{90}}{3m^2}\frac{\partial f_0}{\partial x}. \quad (9)$$

Substituting f_0 from eq. (8) we obtain

$$\{\Gamma, Q\} = -\frac{1}{4\pi}\left(\frac{\lambda_{90}}{3m\lambda_\varepsilon}\right)^{1/2} \int dx' nT^{-1/2}\{1, T\} \times \left\{\{I(\theta), K(\theta)\}\frac{\partial T}{\partial x'} - \{J(\theta), L(\theta)\} \times \left(\frac{5}{2}\frac{\partial}{\partial x'}\frac{T}{} - \frac{T}{n}\frac{\partial n}{\partial x} + T\frac{\partial}{\partial x'}\left(\frac{(e\phi(x) - e\phi(x'))}{T(x')}\right)\right)\right\} + \frac{\tilde{\delta}_{IB}}{T}\left(\{I(\theta), K(\theta)\}\frac{\partial T}{\partial x'} - \{J(\theta), L(\theta)\} \times \left(\frac{5}{2}\frac{\partial T}{\partial x'} - \frac{T}{n}\frac{\partial n}{\partial x} + T\frac{\partial}{\partial x'}\left(\frac{e\phi(x) - e\phi(x')}{T(x')}\right)\right)\right)\Bigg\} \times \exp[(e\phi(x) - e\phi(x'))/T(x')], \quad (10)$$

where $I(\theta)$, $J(\theta)$, $K(\theta)$ and $L(\theta)$ are the same propagators as described in [8] which are functions of the reduced distance $\theta = \left|\int_x^{x'} dx''/\tilde{\lambda}_s(x'')T^2(x')\right|$. It may be noted here that the Γ and Q expressions are more general than those of the previous model [11], in which the inverse-bremsstrahlung was ignored. The present model also generalizes the work of Luciani *et al.* [6] by self-consistently including the effect of electrostatic potential. This effect manifests itself as an extra exponential term $\exp[(e\phi(x) - e\phi(x'))/T(x')]$ which plays a critical role as we shall see later.

3. Limiting cases

Let us consider the two limiting cases of steep and gentle gradients which illuminate the underlying physics. In the gentle gradient limit, the nonlocal heat flux reduces to the local value because only x' near x would contribute to the integrals of Eq. (10), so that we may let $dx' = T^2\tilde{\lambda}_s$ and perform the θ integrations. The charge neutrality condition (or simply $\Gamma(e\phi) = 0$) gives,

$$\frac{\partial}{\partial x} e\phi(x) = T\frac{\partial}{\partial x}\ln(nT^{5/2} + \tilde{\delta}_{IB} nT^{3/2}). \quad (11)$$

Substituting this value of the electrostatic potential in eq. (10), the local value of heat flux turns out to be

$$Q = (1 + \tilde{\delta}_{IB}/T)Q_{SH}, \tag{12}$$

where $Q_{SH} = -25.532n\ (T/m)^{1/2}\lambda_0(\partial T/\partial x)$ is the classical Spitzer-Härm [14] heat flux value in the high-Z limit of plasma.

On the other hand, for nonlocal case, in which the temperature step from hot to cold is over a distance much shorter than a stopping length, the charge neutrality condition gives the following result,

$$nT^{1/2}(1 + \tilde{\delta}_{IB}/T) \exp\left[(e\phi(x) - e\phi(x'))/T(x')\right] = C, \tag{13}$$

where the constant of integration, C, may be obtained by using the condition that nonlocal potential becomes local for gentle gradients,

$$e\phi(x') = e\phi(x) + T \times \ln\left[nT^{1/2}(1 + \tilde{\delta}_{IB}/T)/n_c\, T_c^{1/2}(1 + \tilde{\delta}_{IB}/T_c)\right]. \tag{14}$$

Finally, the maximum heat flow expression becomes

$$Q_{max} = 6\left(\frac{\lambda_{90}}{3\pi m\lambda_c}\right)^{1/2} n_c\, T_c^{1/2}(T_H - T_c)\frac{\Gamma(5/4)}{\Gamma(7/4)}(1 + \tilde{\delta}_{IB}/T_c), \tag{15}$$

where the subscripts c and H denote cold and hot species of electrons, respectively and $\tilde{\delta}_{IB}$-term represents the inverse-bremsstrahlung absorption effect.

4. Results and discussion

In this paper, we have investigated the effect of inverse-bremsstrahlung absorption on nonlocal heat transport. This effect is of fundamental importance in the laser-plasma interaction experiments near the critical density surface since it determines the structure of the density and temperature profiles. We have found that the inverse-bremsstrahlung absorption effect which is represented by $\tilde{\delta}_{IB}$, enhances the heat flux. The same has also been observed in the Fokker-Planck numerical simulations of Matte *et al.* [3] and which this is precisely what $\tilde{\delta}_{IB}$-term in eqs. (12) and (15) represents. In the absence of local inverse-bremsstrahlung absorption (i.e., $\tilde{\delta}_{IB} \to 0$) our previous results of [11] are completely recovered. Mirza *et al.* [11] showed how the electrostatic potential modifies the earlier results of Albritton *et al.* [8]. For example, the charge neutrality condition does not give just a constant factor as in the local Spitzer-Härm theory but varies spatially when the transport becomes nonlocal. Furthermore, in the steep gradient limit the temperature dependence of the maximum heat flow expression also changes substantially.

The results concerning the effect of inverse-bremsstrahlung absorption on heat transport are straightforward to understand. The effect can simply be presented by multiplying the usual results by factor $(1 + \tilde{\delta}_{IB}/T_c)$ in the region in which a laser light is propagating. If we choose typical laser wavelengths λ, intensities, I, and the temperature at the critical density surface, T_H, as described by Bendib *et al.* [9], we find that the value of the $(1 + \tilde{\delta}_{IB}/T_c)$ term at the critical density lies between (1.016–1.116) as shown in Table I and, consequently, the value of the flux limiting factor, f, lies between 0.15–0.17. Table II compares the value of $f(= Q_{max}/Q_{FS})$ for various models, using typical parameters $Z = 4$, $T_H = 2T_c$ and $n_H = n_c$ where $Q_{FS} = n(T_H^3/m)^{1/2}$. Our result compares favourably with the Fokker-Planck simulation results of Bendib et al. [9] and Matte et al. [3]. On the other hand, in the absence of inverse-bremsstrahlung process and in the local limit, the classical Spitzer-Härm expression of heat flux is completely recovered.

Table I. *Value of the inverse bremsstrahlung term and the flux inhibition factor f for various laser wavelengths, intensities and temperatures at the critical surface for* $Z = 4$, $T_H = 2T_c$, $n_H = n_c$ *and* $\ln \Lambda_{ee} = \ln \Lambda_{ei}$

$\lambda(\mu m)$	$I(10^{14}$ W/cm$^2)$	T_H (keV)	$(1 + \tilde{\delta}_{IB}/T_c)$	f
1.06	3	2.3	1.07	0.163
1.06	6	2.8	1.116	0.17
0.353	4.5	1.7	1.016	0.155
0.353	10	2.4	1.025	0.156

Table II. *Flux inhibition factor f as proposed by different nonlocal models for* $Z = 4$, $T_H = T_c$, $n_H = n_c$ *and* $\ln \Lambda_{ee} = \ln \Lambda_{ei}$

f	Model
0.15	Matte *et* al. [3] – simulation results with inverse-bremsstrahlung effect.
0.21	Luciani *et al.* [15] – nonlocal model result.
0.46	Albritton *et al.* [8] – nonlocal model result.
0.15	Bendib *et al.* [9] – simulation result.
0.15–0.17	Our results with inverse-bremsstrahlung absorption term

Acknowledgements

This work was partially supported by the PAEC Project and the PSF Project C-QU/Phys(69), Islamabad, Pakistan.

References

1. Albritton, J. R., Phys. Rev. Lett. **50**, 2078 (1983).
2. Langdon, A. B., Phys. Rev. Lett. **44**, 575 (1980).
3. Matte, J. P., Johnston, T. W., Delettrez, J. and McCrory, R. L., Phys. Rev. Lett. **53**, 1461 (1984).
4. Bell, A. R., Evans, R. G. and Nicholas, J., Phys. Rev. Lett. **46**, 243 (1981).
5. Mason, R. J., Phys. Rev. Lett, **47**, 652 (1981).
6. Luciani, J. F., Mora, P. and Virmont, J. Phys. Rev. Lett. **51**, 1664 (1983).
7. Luciani, J. F., Mora, P. and Pellat, R., Phys. Fluids **28**, 835 (1985).
8. Albritton, J. R., Williams, E. A., Bernstein, I. B. and Swartz, K. P., Phys. Rev. Lett. **57**, 1887 (1986).
9. Bendib, A., Luciani, J. F. and Matte, J. P., Phys. Fluids **31**, 711 (1988).
10. Kishimoto, Y., Mima, K. and Haines, M. G., J. Phys. Soc. Japan **57**, 1972 (1988).
11. Mirza, A. M., Murtaza, G. and Qaisar, M. S., Phys. Lett. A. **141**, 56 (1989).
12. Kidder, R. E., "Physics of High Energy Density" (Academic, New York, 1971).
13. Deck, D., Laser and Particle Beams **5**, 49 (1987); NRL Plasma Formulary 1987.
14. Spitzer, L. and Härm, R., Phys. Rev. **89**, 977 (1953).
15. Luciani J. F. and Mora, P., Phys. Lett. A. **116**, 237 (1986).

Physica Scripta. Vol. 47, 814–816, 1993

Sequential Focusing in a Mather-Type Plasma Focus

M. Nisar, F. Y. Khattak, G. Murtaza, M. Zakaullah and N. Rashid

Department of Physics, Quaid-i-Azam University, Islamabad 45320, Pakistan

Received November 17, 1992; accepted January 19, 1993

Abstract

The current sheath behavior in a small 3 kJ plasma focus device, in the presence of a target placed downstream of the anode is investigated. The voltage signal and the sequential bursts of neutrons give a clear indication of the occurrence of the sequential focusing.

1. Introduction

Plasma focus has been the subject of intensive research for decades due to its potential for high neutron yield under optimum conditions and this device can act as a source of intense pulsed X-rays. Recently interest has been shown in using the plasma focus device as a cascading focus device [1, 2] by placing a target downstream of the anode. Such a device may have practical applications for the production of sequential bursts of neutron and soft X-ray for various purposes like neutron radiography and soft X-ray cinematography.

After the breakdown in a Mather-type plasma focus, the current sheath moves along in the axial run down phase, sweeping the mass in its front until it collapses in the radial phase. When focusing occurs, a rapid compression of plasma takes place. The strong electro-mechanical action draws energy from the magnetic field, pumping the energy into the compressing plasma. This mechanism results in a distinctive current dip and a voltage spike. A bigger spike in the voltage signal and a dip in the current signal are indications of strong focusing. In the presence of the target, after the collapse, the current sheath climbs over the target which now acts as a second anode as shown in Fig. 1. Hence the sheath now runs along the second axial phase until it collapses. Moo *et al.* [3] have studied the effect of using metal obstacles and deuterated targets downstream the current sheath on the ion beam and neutron yield in a small plasma focus device. The behavior of the current sheath in the presence of the target was shadowgraphically studied by Lee *et al.* [1]. In their arrangement, the supporting rod with the insulating glass tube posed a problem to the cascade focusing beyond the target. In this paper we report on the experimental evidence of sequential focusing in a low energy focus device, with a unique target insertion mechanism, by the analysis of the high voltage signal and the neutron pulse.

2. Experimental arrangement

These experiments were carried out in a low energy (3 kJ) focus device [4] energized by a single capacitor. The electrodes system is comprised of the inner copper anode, having a diameter of 18 mm and length of 152 mm and the outer electrode, consisting of six copper rods. Figure 2 shows the hanging target and the electrodes system. The target, in our case, is a copper disc having a thickness of 5 mm and a diameter of 35 mm. The thickness of the target has a crucial role since the current sheath, after climbing the target, must have enough time to become uniform before reaching the subsequent focus event. The target is hanged from the top flange of the chamber with the help of two supporting rods. These supporting rods are 3 mm thick brass rods encapsulated in glass tubes. The target can then be placed at the floating potential at various axial positions from the end of the anode or be withdrawn to the rear of the chamber without interrupting the vacuum in the chamber. Our target insertion mechanism allows enough room to the current sheath to focus beyond the target.

A resistive voltage divider with a response time of 15 ns is strapped across the anode collector plate and the cathode collector plate to measure the voltage across the focus tube. A channel of a dual channel 100 MHz oscilloscope is used

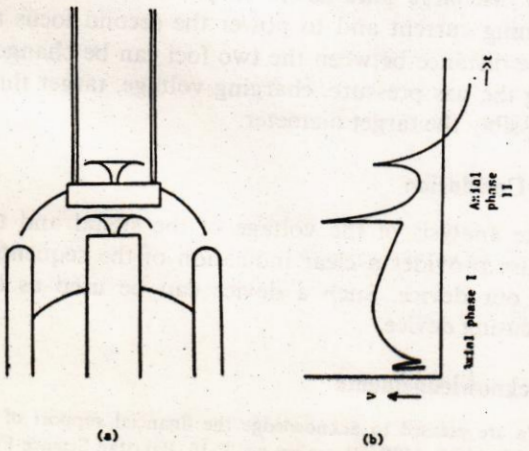

Fig. 1. Schematic layout of the sequential focusing event. (a) Cascading anode; (b) Sequential voltage spike

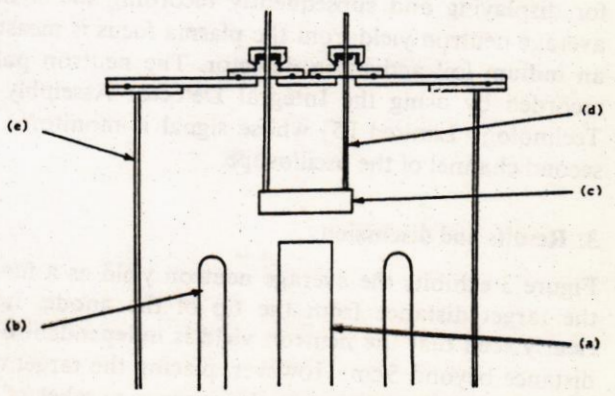

Fig. 2. Schematic diagram of the plasma focus electrodes and target. (a) Copper anode; (b) Copper cathodes; (c) Copper target, 3.5 cm dia.; (d) Supporting rods; (e) Chamber

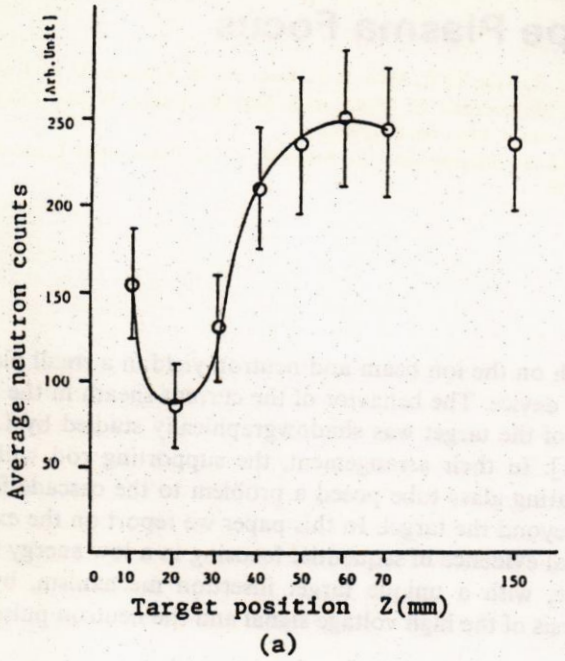

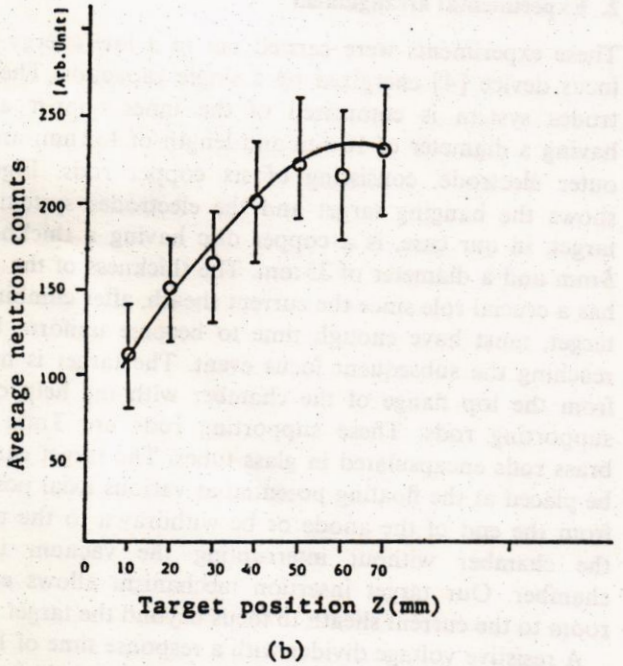

Fig. 3. Average neutron yield as a function of target distance from the tip of the anode, (a) without hole and (b) with a hole in the center of the target

for displaying and subsequently recording the signal. The average neutron yield from the plasma focus is measured by an indium foil activation detector. The neutron pulse was recorded by using the Integral Detector Assembly of NE Technology Limited [5] whose signal is monitored on the second channel of the oscillosope.

3. Results and discussion

Figure 3 exhibits the average neutron yield as a function of the target distance from the tip of the anode. It can be clearly seen that the neutron yield is independent on target distance beyond 5 cm. However, placing the target closer to the anode surface decreases the average number of neutron counts and a minimum is obtained at a distance of about 2 cm, which is in agreement with the results obtained by Moo *et al.* [3]. The reduction in the neutron yield, when

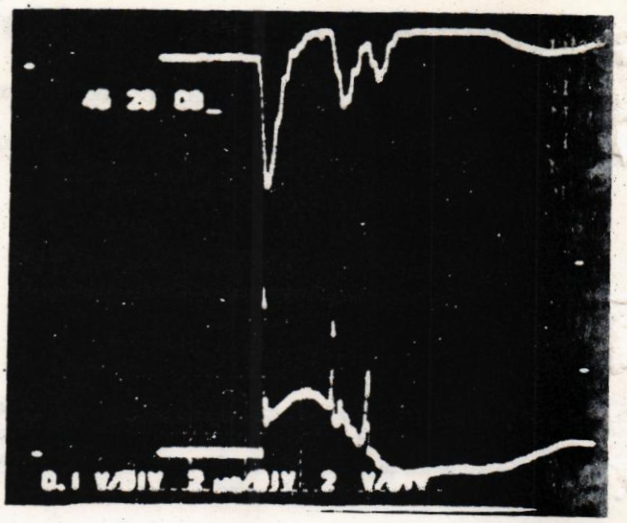

Fig. 4. A typical oscillogram of the voltage probe signal and the neutron pulse. The distance of the target from the tip of the anode is 1.0 cm, and the D2 pressure is 2.5 mb. The baseline time is 2 μs per division. The top signal is the neutron pulse and the bottom one shows the voltage probe signal

compared with the situation when no target is used, is due to the interference of the target with the deutron beam accelerated downstream outside the focus region. This is confirmed by replacing the target with a copper disc of the same size having a 2 mm hole at its center. Figure 3(b) shows the average neutron yield as a function of target distance (target with a hole at its center). The average neutron yield has increased significantly even for a distance of 2 cm. In this case the neutron beam generated in the focusing column due to the $m = 0$ instability passes through the hole and then, due to the target mechanism, appreciable neutrons are produced.

Interestingly it is observed that by bringing the target even closer to the anode, at a distance of about 1–1.2 cm, the average neutron yield increases abruptly. Moreover a second spike is also observed in the voltage signal and in the neutron pulse as can be seen in the oscillogram shown in Fig. 4. This second spike is a clear indication of a second focus after the target. The second focus is at about 1 μs interval from the first focus shown by the second spike in the two signals. The second spike is relatively low, implying a weak second focus. However, it proves that such a device can possibly be used as a cascading focus device to produce bursts of neutrons and soft X-ray. It is necessary to adjust the discharge parameters to provide sufficiently long sustaining current and to power the second focus adequately. The distance between the two foci can be changed by altering the gas pressure, charging voltage, target thickness and possibly the target diameter.

4. Conclusion

The analysis of the voltage of the signal and the neutron pulse provides a clear indication of the sequential focusing in our device. Such a device can be used as a cascading focusing device.

Acknowledgements

We are pleased to acknowledge the financial support of PAEC, ICAC-QAU, UGC, NSRDB project no. P-16, Pakistan Science Foundation Project Nos. C-QU/Phys(69), (70), (75) and Dr. A. Q. Khan research laboratory.

References

Lee, S., Alabraba, M. A., Gholap, A. V., Kumar, S., Kwek, K. H., Nisar, M., Rawat, R. S. and Sing, J., IEEE Trans. Plasma Sci. **19**, 912 (1991).

Lee, S., IEEE Trans. Plasma Sci. **19**, 912 (1991)

Moo, S. P., Chakrabarty, S. K. and Lee, S., IEEE Trans. Plasma Sci. **19**, 515 (1991).

4. Lee, S., Tou, T. Y., Moo, S. P., Eissa, M. A., Gholap, A. V., Kwek, K. H., Mulyodrono, S., Smith, A. J., Suryadi, Usada, W. and Zakaullah, M., Am. J. Phys. **56**, 62 (1988).
5. Manual, Integral Detector Assembly of NE Technology Limited, Dec. 1990.